STUDY OF $CaSO_3 \cdot 1/2H_2O$ NUCLEATION AND GROWTH RATES IN SIMULATED FLUE-GAS DESULFURIZATION LIQUORS

by

Brian John Kelly

A Thesis Submitted to the Faculty of the

DEPARTMENT OF CHEMICAL ENGINEERING

In Partial Fulfillment of the Requirements
For the Degree of

MASTER OF SCIENCE

In the Graduate College

THE UNIVERSITY OF ARIZONA

1 9 8 3

STATEMENT BY AUTHOR

This thesis has been submitted in partial fulfillment of requirements for an advanced degree at The University of Arizona and is deposited in the University Library to be made available to borrowers under rules of the Library.

Brief quotations from this thesis are allowable without special permission, provided that accurate acknowledgment of source is made. Requests for permission for extended quotation from or reproduction of this manuscript in whole or in part may be granted by the head of the major department or the Dean of the Graduate College when in his judgment the proposed use of the material is in the interests of scholarship. In all other instances, however, permission must be obtained from the author.

SIGNED: Brian J Tully

APPROVAL BY THESIS DIRECTOR

This thesis has been approved on the date shown below:

A. D. Randolph
A. D. RANDOLPH
Professor of Chemical Engineering

4/4/83
Date

What has been, that will be;
What has been done, that will be done.
Nothing is new under the sun.

Even the thing of which we say, "See,
this is new!" has already existed in the
ages that preceded us.

Ecclesiastes 1:9-10

ACKNOWLEDGMENTS

The author wishes to thank his advisor, Professor Alan D. Randolph, for his support, encouragement, and intuition throughout this work. The author also wishes to thank his wife. Her patience and understanding made everything possible.

The author is grateful to the Electric Power Research Institute, Inc. (EPRI) for financial support under contract number RP1030-3. The following legal notice is required by EPRI.

This work was prepared by The University of Arizona as an account of work sponsored by EPRI. Neither EPRI, members of EPRI, nor The University of Arizona, nor any person acting on behalf of either:

a. Makes warranty or representation, express or implied, with respect to the accuracy, completeness, or usefulness of the information contained in this report, or that the use of any information, apparatus, method, or process disclosed in this report may not infringe on privately owned rights.

b. Assumes any liabilities with respect to the use of, or for damages resulting from the use of, any information, apparatus, method, or process disclosed in this report.

TABLE OF CONTENTS

LIST OF ILLUSTRATIONS

LIST OF ILLUSTRATIONS -- Continued

LIST OF TABLES

ABSTRACT

The purpose of this study was to investigate various methods of increasing $CaSO_3 \cdot 1/2H_2O$ crystal size in flue-gas scrubber liquors. The methods studied were: 1) growth and nucleation modification through the use of trace chemical additives, and 2) computer simulation of different crystallizer configurations.

Metastability tests were made to scan eight chemical additives. The most active compounds were NMTP and citric acid. These additives were used in MSMPR experiments to determine calcium sulfite growth and nucleation kinetics. Calcium sulfite was found to precipitate as a Class II system. The presence of citric acid resulted in increased nucleation rates in the continuous crystallizer.

A crystallizer simulation program was used to explore sensitivity of product size to variations in product classification and removal rate. By decreasing clarifier cut size and employing a "Double Draw-Off" product removal configuration, it was predicted that product size would increase by a factor of two over that of existing scrubber precipitators.

CHAPTER 1

INTRODUCTION

Recent trends to shift from oil- to coal-fired plants for electric power generation have resulted in the need to develop effective and reliable methods for the removal of SO_2 from stack gases. Presently, the most common commercial process is the lime/limestone scrubber. In this process, the absorption of SO_2 from stack gases is achieved by contacting the flue gas with a lime or limestone slurry. The absorption of SO_2 results in the formation of a supersaturated solution of calcium ions and sulfite ions or, if excess air is supplied, sulfate ions. The calcium sulfite-sulfate is precipitated as a fine solid and is disposed of as landfill. A typical scrubber configuration is shown in Figure 1.

The ability to produce larger sized crystals is of importance from the standpoint of product dewaterability and eventual deposition as a stable landfill material. A small crystal product requires large clarifiers and filters. A calcium sulfate product generally consists of larger crystals than those of calcium sulfite. However, the added capital expense of installing an oxidation tank for conversion of the sulfite ion may not be justified if a cost-effective method for producing a larger calcium sulfite product is discovered. The purpose of this study was two-fold:

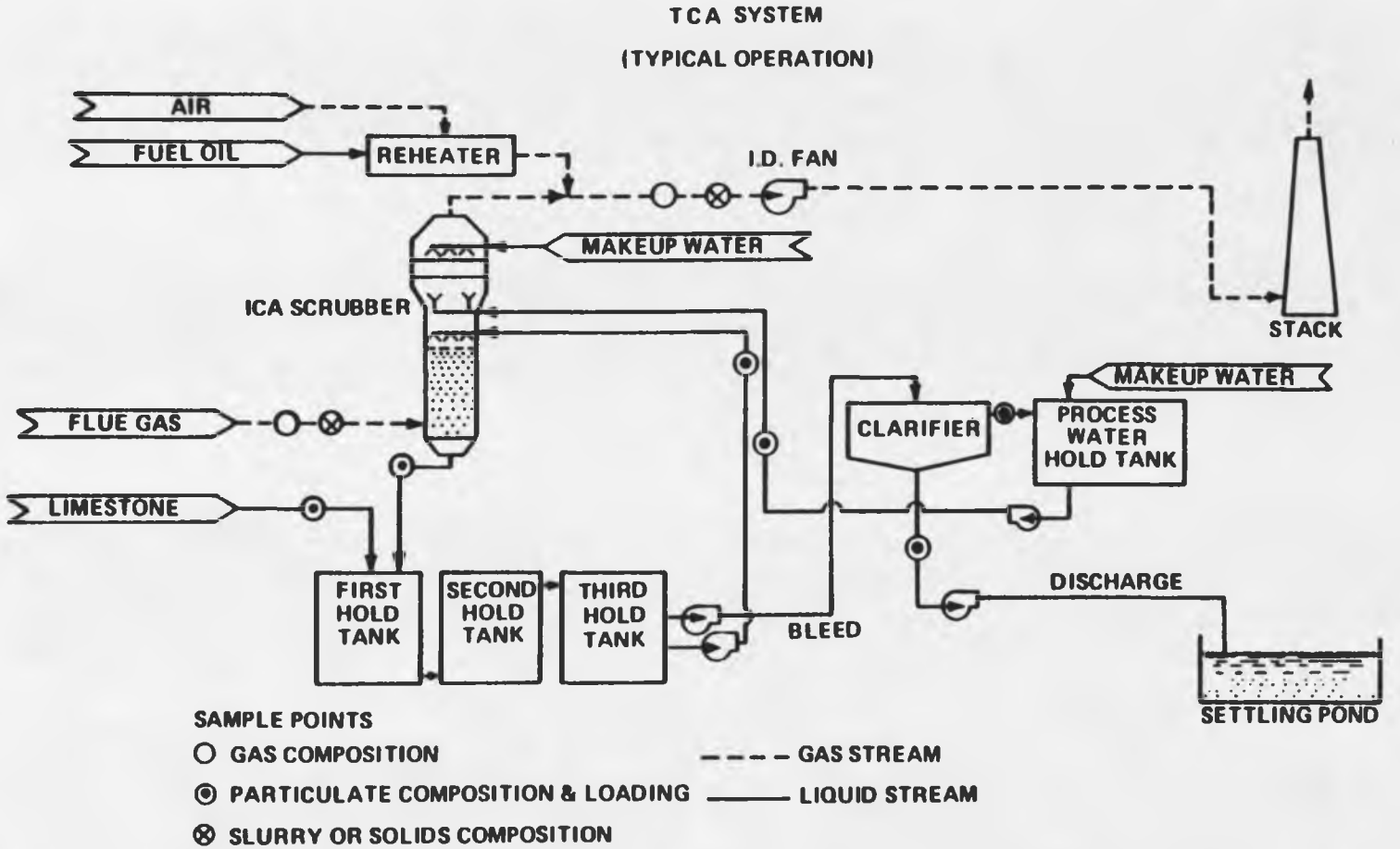

Figure 1. Flow Diagram of Typical Scrubber.

1. To compare the relative effects of various chemical additives on size and morphology of calcium sulfite hemihydrate crystals.
2. To determine crystallization kinetics of calcium sulfite hemihydrate using an MSMPR crystallizer configuration. Once determined, the kinetic parameters were used in a crystallizer simulation to indicate how crystallizer design might be used to improve product size.

All experiments were carried out in a 240 ml well-mixed crystallizer.

Comparison of various chemical additives was performed in batch experiments using the "Up and Down" statistical method introduced by Dixon and Mood (1948) and later modified for small samples by Brownlee, Hodges, and Rosenblatt (1953). A simulated flue gas desulfurization (FGD) liquor containing calcium, magnesium, potassium, chloride, sulfite, and sodium ions was mixed with trace quantities of the chemical additives studied. The relative effects of the various additives were compared by recording the solution supersaturation necessary to obtain observable calcium sulfite crystals in a waiting time of exactly 15 minutes. Observable crystals were classified as those that were large enough to be detected by an in-line, Particle Data Inc. (PDI), particle counter with constant orifice probe size. The chemical additives tested were:

-- Sodium dodecylbenzenesulfonate (SDBS)
-- Citric acid
-- Adipic acid
-- Nitrilotris(methylene)triphosphoic acid (NMTP)
-- Gelatin

-- Sodium oleate

-- Ethylenediamine tetracetic acid (EDTA)

-- Tricaprylylmethylammonium chloride (TCMAC)

Calcium sulfite hemihydrate growth and nucleation kinetics were studied using an MSMPR crystallizer configuration. Two feed solutions were contacted in the crystallizer to produce the required supersaturation. The sulfite feed solution was made up of $NaHSO_3$ and NaOH in water. The calcium feed consisted of a mixture of $CaCl_2$, $MgCl_2$, KCl, and a chemical additive (selected from the previous comparative experiments). Crystallization kinetic parameters were obtained by steady-state crystal size distribution (CSD) analysis. All analyses were performed on the PDI-80xy particle counter and mini-computer.

Kinetic parameters obtained from the MSMPR crystallizer experiments were then used in a previously developed crystallizer simulation program (Nuttall, 1971), the Mark I simulator. The purpose of the simulation was to determine the effect of changes in crystallizer configuration on product CSD. Effects of liquid versus solid residence time and changes in solids residence time as a function of size were studied.

To date, much work has been carried out on characterization and improving stability of flue gas scrubber sludge. Major efforts have been performed by Radian Corporation (Corbett, Hargrove, and Merrill, 1977; Otmers et al., 1974; Jones, Lowell, and Meserole, 1976; Coltharp et al., 1979; Edwards, 1979), Bechtel Corporation (Epstein, 1975; Epstein et al., 1975), the Tennessee Valley Authority (Crowe and Seale, 1979), and The University of Arizona (Randolph and Etherton, 1981; Etherton, 1980; Vaden, 1981). Most studies in the area of solids

formation have been performed as precipitation rate experiments rather than attempting to separate the individual effects of growth and nucleation. This study attempts to define effects of various chemical and physical changes on growth and nucleation rates separately for the $CaSO_3 \cdot 1/2H_2O$ system.

CHAPTER 2

LITERATURE AND THEORY

The crystallization process consists of two major subprocesses:

1. Formation of new crystals from the liquid phase.
2. Growth of existing crystals.

The driving force for both formation and growth of crystals is the liquid phase supersaturation. Variations in the driving force can be used to alter growth and nucleation rates and, hence, crystal habit or morphology.

Nucleation and Growth

Nucleation is the process by which new crystals are formed from a supersaturated liquid phase. There are three types of nucleation mechanisms:

1. Homogeneous nucleation -- the formation of new crystals from the liquid phase as a result of supersaturation alone.
2. Heterogeneous nucleation -- the formation of new crystals in the presence of foreign insoluble material.
3. Secondary nucleation -- the formation of new crystals in the presence of suspended crystals of the same material.

The rate of homogeneous nucleation is described by an Arrhenius-type expression:

$$B^o = C \exp(-\Delta G^*/kT) \quad [1]$$

where

B^o = nucleation rate;

C = proportionality constant;

ΔG^* = free energy of formation of a critical sized nucleus;

k = Boltzman's constant; and

T = absolute temperature.

Heterogeneous nucleation can be described by an equation similar to that for homogeneous nucleation, but with additional terms to account for the decreased energy barrier of crystal formation.

Due to the large roles of crystal-crystal, crystal-impeller, and crystal-wall interactions within an industrial crystallier, secondary rather than homogeneous nucleation is generally the operative mechanism. Clontz and McCabe (1971) demonstrated the effects of crystal-crystal and noncrystal-crystal contact on secondary nucleation. Their results showed that both events gave rise to increased nucleation, although crystal-crystal contact produced the greatest number of nuclei. The number of nuclei formed was also found to be dependent on the solution supersaturation and the level of contact energy. Work performed by Randolph and Larson (1971) indicated that secondary nucleation effects in agitated suspensions undergoing the same energy input can be correlated well by:

$$B^o = k(RPM)\, M_T^{\,j} G^i \quad [2]$$

where

k(RPM) = rate constant, a function of impeller RPM;

M_T = slurry density (mg/liter); and

G = crystal growth rate (μm/min).

Studies conducted by Etherton (1980) on the calcium sulfate system (gypsum) undergoing secondary nucleation gave j = 1.27 and i = 1.48.

Crystal growth is characterized by a two-step mass transfer operation. In the first step, the solute is transported to the crystal surface. Once at the surface, the solute molecule or ion is then integrated into the crystal lattice. With little or no agitation, the growth rate is diffusion-controlled and, hence, proportional to the supersaturation:

$$G = kS \qquad [3]$$

Increased agitation results in increased growth rates until surface integration becomes the controlling growth step. Surface integration of solute ions or molecules takes place at low energy sites or dislocations along the surface of the crystal. Burton, Cabrera, and Frank (1951) indicate that the most probable growth is along screw dislocations which continually generate low energy sites as the dislocation moves across the crystal surface. Screw dislocation growth can be represented by:

$$G = kS^2 \qquad [4]$$

Van Rosmalen (1981) has stated that, for low values of supersaturation, a spiral growth mechanism predominates, while at higher supersaturations growth may be the result of a polynuclear surface nucleation mechanism. This mechanism entails the random formation of nuclei on the originally exposed surface layer and on the surfaces of already growing clusters. The nuclei then expand until they merge with others on the surface or reach the crystal edges. Studies performed by Otmers et al. (1974) on $CaSO_3 \cdot 1/2H_2O$ also showed surface nucleation occurring at high supersaturations. This mechanism cannot be related to the second-order function of supersaturation and, hence, equation [4] may not be valid for all systems. To account for either mechanism, a power-law type expression can be used:

$$G = kS^a \qquad [5]$$

Typically, values of "a" are in the range of 1 to 2. Etherton (1980) observed a kinetic growth constant of 2.2 for calcium sulfate (gypsum).

Crystal Habit Modification

The crystallization process deals with the growth of many small crystals in suspension as well as the formation of new crystals by reacting ions or molecules in solution. The rates of both nucleation and growth depend on the physical and chemical properties of the system. Introduction of various trace additives to a crystallizing system can result in reduced nucleation rates, reduced growth rates, and/or alteration of crystal habit.

The growth rate of a crystal can be considered as an area-average of the growth rates of the individual crystal faces. Faster growing faces or faces with relatively small surface area often grow out of existence by combination with slower growing faces. Van Rosmalen (1981) found this to be the case for gypsum crystals. Addition of a growth inhibitor which is selectively adsorbed on the faster growing faces will retard the growth process and promote the development of these faces over the previously slower growing faces. The inhibition process is not one of complexing with ions in solution, but rather selective adsorption on the crystal surface at active growth sites. This was verified in experiments conducted by van Rosmalen (1981) in which only trace quantities of chemical additives were used.

As was discussed in the previous section, crystal growth occurs at monomolecular steps or dislocations along the crystal surface. Michaels, Brian, and Beck (1964) have reported, for adipic acid crystals, that growth can be retarded by adsorption of trace quantities of SDBS at these sites. The crystal habit modifier acts: 1) to reduce the rate of propagation of the steps across the crystal, or 2) to reduce the generation rate of new surface active sites. The latter effect might be most prevalent when surface nucleation is the growth mechanism.

The generally accepted technique for scanning the effects of various chemical additives on growth and nucleation involves precipitation rate measurements in a seeded continuous flow mixed reactor with increasing feed supersaturation (Otmers et al., 1974; Ottens, 1973; Nývlt et al., 1970; Etherton, 1980). At low inlet supersaturation, the precipitation mechanism will be mainly by growth on existing seed

crystals. As shown in Figure 2, this region has a relatively flat slope and is known as the "metastable zone." As the feed supersaturation is increased, the precipitation rate increases significantly as secondary nucleation becomes the dominant mechanism for solids formation. Studies performed on $CaSO_3 \cdot 1/2H_2O$ by Otmers et al. (1974) showed that the metastable zone extended up to a feed supersaturation of about 3-4 times the solubility product. For gypsum, they found that the metastable zone extended to approximately 1.3-1.4 times the solubility product.

The metastable limit for homogeneous nucleation can be determined by particle counting techniques. As in this study, the detection of a minimum number of particles of given size determines the metastable limit. Since this criterion is a function of the minimum detectable crystal size and number, the metastable limit will depend on the ability of the particle detection system. However, for identical methods of determining the metastable zone width, the effect of seeding (and, hence, secondary nucleation) is to decrease the metastable limit, as shown in Figure 2.

In nucleation experiments, experience shows that there is a waiting time between the attainment of supersaturation and the appearance of crystals as visible particles. This waiting time is defined by Melia (1965) to consist of three parts as shown below:

$$t = t_i + t_n + t_g \qquad [6]$$

where

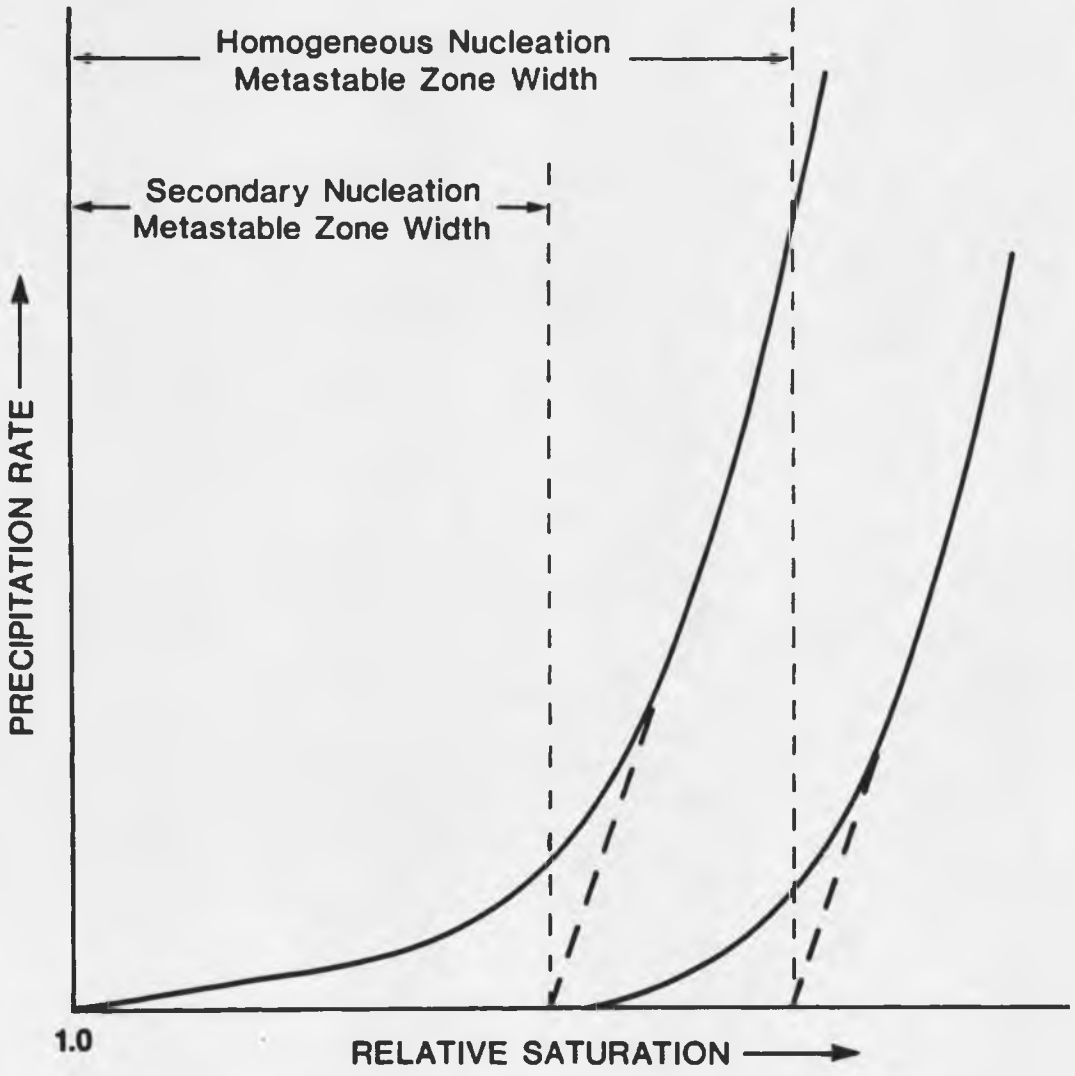

Figure 2. Typical Metastable Zone Width Measurement.

t_i = time required for the attainment of the embryo distribution characteristic of the supersaturated condition;

t_n = time required for nucleus formation; and

t_g = time for growth of nucleus to measurable size.

Melia (1965) has stated that, from the steady-state theory of nucleation:

$$t_g << t_n > t_i$$

However, a steady-state experiment would be conducted at constant supersaturation. A batch experiment results in an ever-decreasing supersaturation due to relief caused by both initial nucleation and subsequent growth of the initial nuclei to detectable sizes. Since it was shown that growth rate can be represented as a power function of supersaturation, G for a batch-type experiment will continually decrease with time. In this case, it is postulated that $t_g >> t_n$ since the initial nucleation would occur at the highest supersaturation and subsequent growth would occur with somewhat less driving force.

To quantitatively test the effect of various chemical additives on crystal growth rate, a series of batch experiments can be conducted. Based on the above postulate that $t_g > t_n$, the time measured between the attainment of supersaturation and the time at which crystals can be detected is approximately equal to t_g. For a set of batch experiments with equal concentrations of chemical additives, the supersaturations required to obtain the same t_g can be used to compare the relative crystal growth retardation caused by each of the additives. A high

initial supersaturation is indicative of a depressed growth rate. Alternatively, the experiment can be interpreted as measuring the true retardation of nucleation, t_n.

To account for the statistical nature of a nucleation event, a series of experimental runs for each chemical additive should be made. A method for analyzing this type of statistical experiment is given by Dixon and Mood (1948) and has been modified for small samples by Brownlee et al. (1953). This method, called the "Up and Down Statistical Method," consists of applying a stimulus to a system and noting the existence of a desired response. In the case of nucleation, the stimulus would be initial solution supersaturation or concentration of limiting reagent. The desired response would be detection of particles at $t = t_g$ (or t_n). The level of stimulus of a run is based on the response of the previous run: a positive response in the previous run results in a decreased stimulus level applied to the next run. The reverse is true for a negative response in the previous run. In this manner, a statistical distribution of the required supersaturation to just detect crystals at a predetermined time, t_o, is obtained.

The Up and Down Method depends on a log-normal distribution of data with equally spaced stimuli. The type of distribution under investigation is similar to that obtained by dropping explosives from different heights, discussed by Dixon and Mood (1948). They indicate that this type of distribution can be forced normal by taking the logarithm of the stimuli levels. This, however, causes equal-spaced linear stimuli levels to be logarithmically spaced. It can be shown

that, for large levels of stimuli and small linear spacing, the logarithmic spacing is also approximately constant.

From Brownlee et al. (1953), the average for the normal distribution can be estimated from:

$$\hat{\mu} = C/N = \log \text{ average concentration} \qquad [7]$$

where

$$C = \sum_{n=2}^{N+1} \log (SO_3^{=} \text{ concentration});$$

n = run number (n = 1 is defined by the first run in which an opposite response is obtained in the immediately following run); and

N = total number of runs made beginning at n = 1.

The actual average concentration of limiting reagent is then obtained from:

$$\overline{\text{Conc.}} = 10^{\hat{\mu}} \qquad [8]$$

Wey and Jagannathan (1982) have shown that the relative supersaturation and, hence, the growth rate seen by each of the crystal faces associated with a polyhedral crystal is a function of the equilibrium (solubility) concentration for each face. This equilibrium concentration is not constant for all crystal faces, but varies with the surface roughness on an atomic scale. This is consistent with work performed by van Rosmalen (1981).

For growth normal to a crystal face of area A_i, an average crystal growth rate is defined by Matuchová and Nývlt (1976) as:

$$G = \frac{\Sigma G_i A_i}{\Sigma A_i} \qquad [9]$$

where subscript i refers to the ith crystal face. Thus, growth inhibition at any or all of the crystal faces of a polyhedral crystal will reduce the average growth rate for the entire crystal. To alter growth on a cationic surface of an ionic crystal, use of an anionic surface active agent is warranted. The reverse is true for an anionic crystal surface. This has been verified by Michaels and Colville (1960) and Michaels et al. (1964). Verification of the actual effects of the chemical additive on the individual crystal faces can only be ascertained through SEM measured growth rates. Measurement of the individual crystal face growth rates was not within the scope of this study. Only those chemical additives which exhibited the greatest effect on the metastable zone width were used in later MSMPR experiments.

Population Balance

The crystallization process can only be described adequately in terms of a population balance. The population balance accounts for particles entering and leaving the system as well as growth and breakage of existing particles. The population balance as derived by Randolph and Larson (1971) is given by:

$$\frac{\partial n}{\partial t} + \frac{\partial (Gn)}{\partial L} + n \frac{\partial (\log V)}{\partial t} = - \sum_i \frac{n_i \bar{Q}_i}{V} + B(L) - D(L) \qquad [10]$$

For the steady-state MSMPR crystallizer with no crystal breakage and clear feed liquor, the equation describing the population distribution is:

$$n(L) = \frac{B^o}{G} \exp\left\{-\frac{L}{G\tau}\right\} \qquad [11]$$

where

n(L) = population density (number/cc-micron);

G = linear growth rate (micron/min);

B^o = nucleation rate (number/cc-min);

L = linear particle size (micron); and

τ = residence time (min).

To obtain the cumulative number distribution of particles larger than size L, equation [11] must be integrated between size L and infinity:

$$N_L = B^o\tau \exp\left\{-\frac{L}{G\tau}\right\} \qquad [12]$$

where N_L = number of particles of size greater than size L. This equation predicts that a plot of $\ln(N_L)$ versus L will give a straight line with slope of $-1/G\tau$ and an intercept of $B^o\tau$. Either equation [11] or [12] can be used to regress population data to obtain B^o and G.

CHAPTER 3

EXPERIMENTAL

The experimental apparatus used in this study was largely designed by Particle Data Inc. in conjunction with Dr. Alan D. Randolph from The University of Arizona. The PDI "mini-nucleator" is a 240-ml, jacketed glass vessel designed to attach directly to the PDI-80xy particle counter. This configuration makes it possible to perform in-line particle measurement and analysis. The mini-nucleator is equipped with a variable speed glass impeller, draft tube, and constant liquid level control. Figure 3 is a schematic of the PDI mini-nucleator.

The PDI-80xy uses the zone sensing principle to determine the number and size of particles in solution. The principle consists of measuring current variations between two electrodes located on either side of an orifice. Particles suspended in an electrolyte solution are drawn through the orifice with a vacuum pump. As the particle passes through the orifice, the resistance of the solution at the orifice changes. This is registered as a pulse whose amplitude is proportional to the particle volume. The particle volume is then converted to an equivalent linear size (spherical diameter) and a histogram of number of particles versus size is displayed on the PDI Elzone^{R} Monitor (oscilloscope). The raw data can then be manipulated using the 80xy and accompanying printer/terminal. The PDI-80xy is equipped with an MSMPR

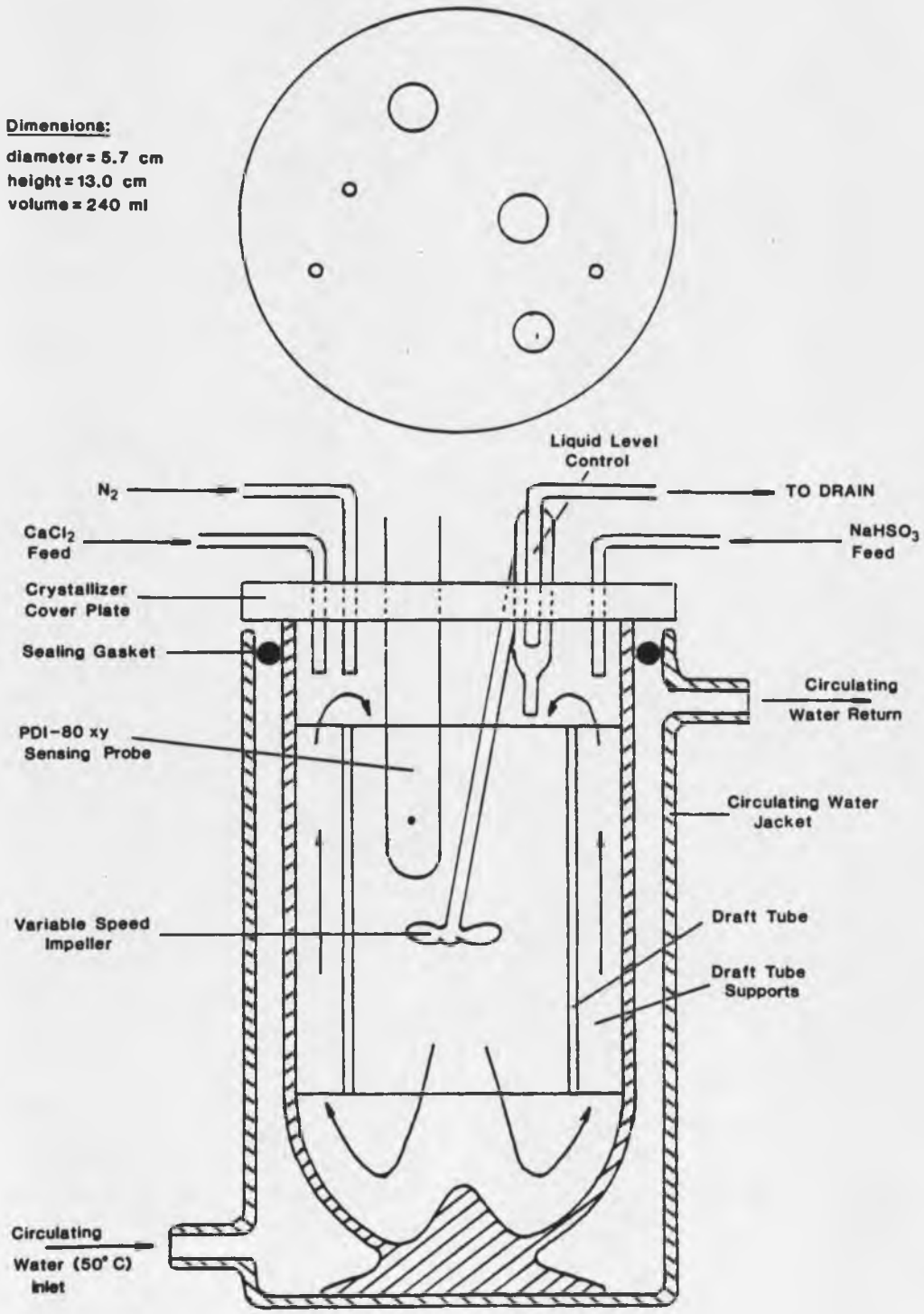

Figure 3. Particle Data Inc. "Mini-Nucleator" with In-Line Particle Data Analysis.

crystallization program which plots cumulative number versus size per equation [12]. This plot is used to determine CSD and kinetic parameters. Figure 4 is representative of a typical output.

Comparison of Chemical Additives

Apparatus

The study of the effects of the various chemical additives was conducted with the mini-nucleator connected directly to the PDI-80xy. The draft tube and liquid level controller were removed to create a well-mixed batch tank configuration. Agitation was produced with a 2.4-cm diameter glass impeller.

To prevent secondary nucleation, both feed solutions were passed through pre- and final filters. The pre-filter was a Pall DFA 3001BP, 3.0 micron absolute filter. The final filter was a Pall DFA 3001AR, 0.2 micron absolute filter. The mini-nucleator was maintained at a constant temperature by circulating water supplied by a Haake model EE temperature controlled bath. To prevent sulfite oxidation, it was necessary to maintain a nitrogen blanket above the sulfite feed tank and mini-nucleator at all times.

Procedure

The metastable limit experiments were carried out using the experimental apparatus and setup shown in Figure 5. Known volumes of $NaHSO_3$ (buffered with NaOH) and $CaCl_2$ (with $MgCl_2$, KCl, and chemical additive) feed solutions were metered to the 200 ml working volume

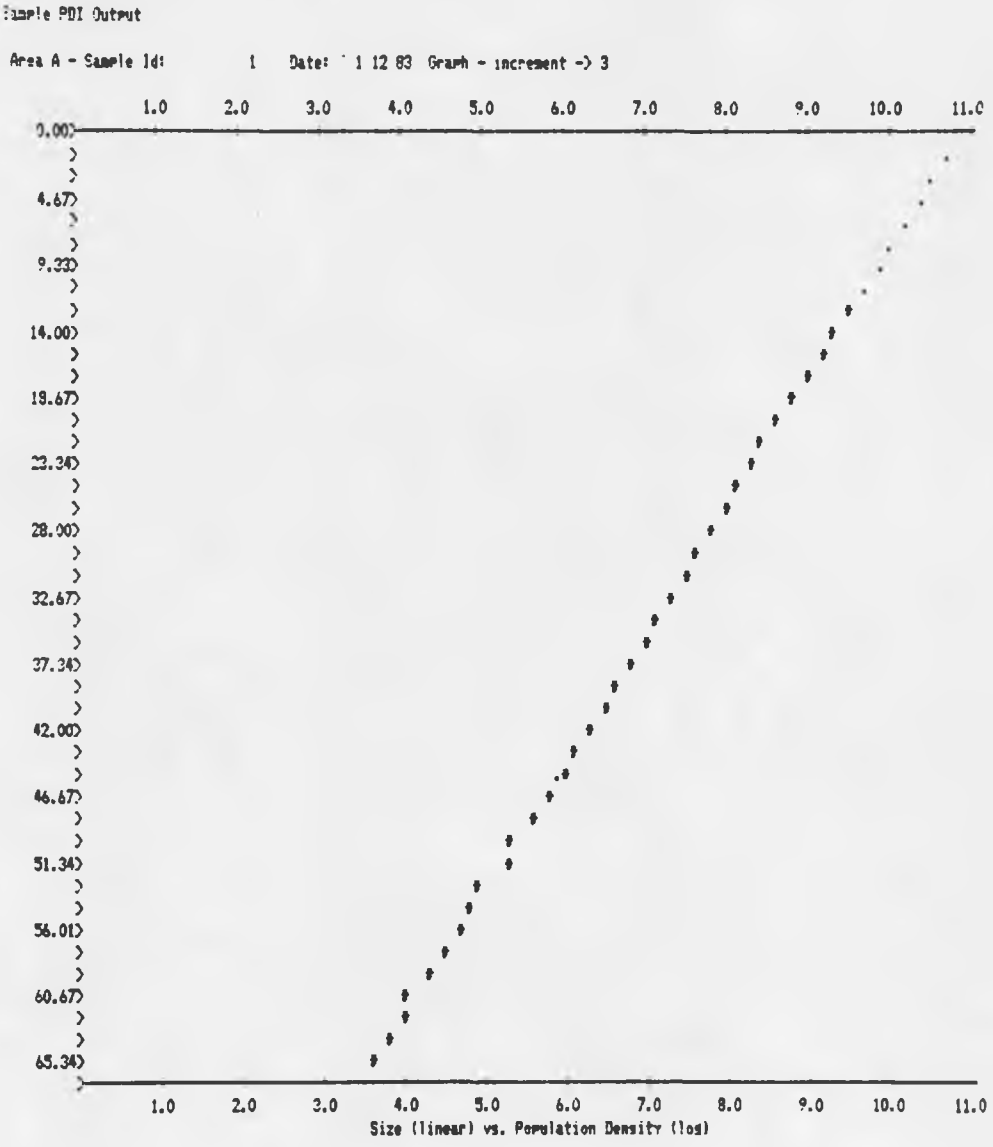

Correlation Coefficient = 0.82
Intercept = 10.146, Slope = -0.102 log(no./cc)/micrometer
Tau = 15.000 min., Rho = 2.535 Grams/cc.
B0 = 1699 no./cc-min.
G = 0.66 microns/min.
Population-average size = 9.84 microns
Weight-average = 39.357 microns
MT = 1.933000e+02 grams/cc.
Nuclei density = 2590 no./cc.-microns

Figure 4. Typical PDI-80xy Output.

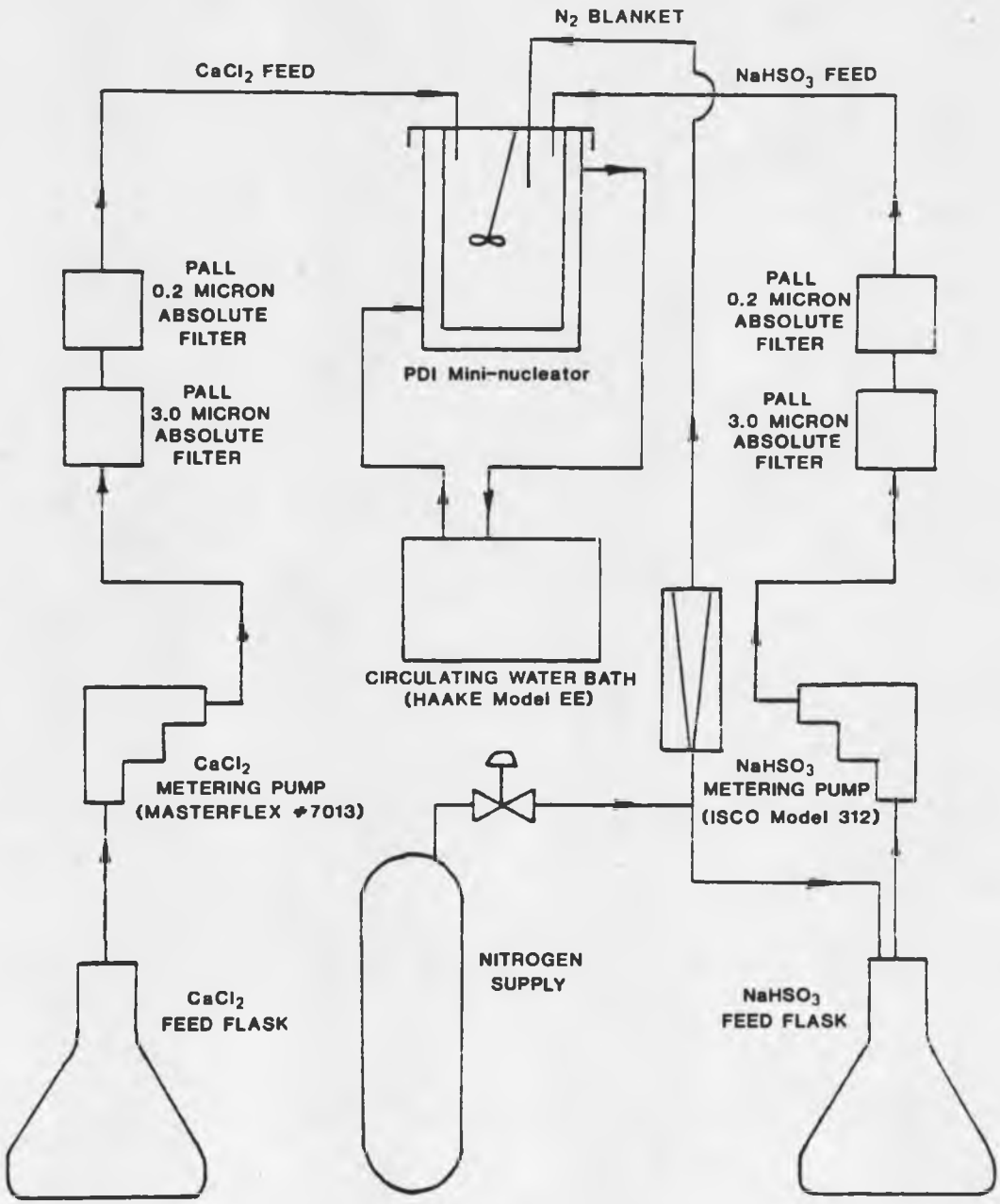

Figure 5. Metastable Limit Experimental Flow Diagram.

crystallizer. The crystallizer was maintained at 50°C and continually agitated at a stirrer rate of approximately 650 RPM.

Prior to each set of experimental runs, the $CaCl_2$ feed flask was filled with 1 liter of aqueous $CaCl_2$ feed solution containing: 98.49 gm $CaCl_2 \cdot 2H_2O$, 25.09 gm $MgCl_2 \cdot 6H_2O$, 3.15 gm KCl, and chemical additive. The $CaCl_2$ feed concentrations were selected to produce crystallizer concentrations in agreement with those found in Epstein's (1975) "Limestone Reliability Verification Tests." The $CaCl_2$ feed flask was continually stirred throughout the experiment.

The $NaHSO_3$ feed flask was filled (under nitrogen purge) with 1.8 liters of aqueous solution containing: 46.84 gm $NaHSO_3$ and 5.4 gm NaOH.

Prior to each individual run, the crystallizer was detached from the 80xy stand, rinsed, and washed with hot soapy water. The crystallizer was then rinsed with distilled H_2O filtered to 0.2 microns absolute. It was then filled with the same water to the predetermined volume. The circulating water bath was connected and the crystallizer allowed to heat up for 15 minutes.

During the heat up period, the 80xy probe, electrode, and stirrer were rinsed with 1% H_2SO_4, rinsed with distilled filtered H_2O, and immersed in hot filtered distilled H_2O. The probe was then flushed with 1% NaCl solution.

After the 15 minute heat up period, the feed lines were purged with a few milliliters of solution. The crystallizer was placed back on the 80xy stand. The $CaCl_2$ feed pump was started and allowed to run for 32 seconds (25 ml/min). The crystallizer was allowed to heat up for an

an additional 5 minutes. The $NaHSO_3$ feed pump was started and run for the predetermined time (depending on the results of the previous run, either 5 seconds longer or 5 seconds shorter) at a rate of 6.67 ml/min. The crystallizer was then mixed for 15 minutes prior to sampling with the PDI-80xy. The criterion used for the detection of crystals was a PDI register of greater than 30 counts using a 150 micron orifice and a 2.0 ml volumetric section (sample volume). With a 150 micron orifice, detection of particles down to a size of approximately 5-6 microns is possible.

Results

The results of the metastable limit experiments are shown in Table 1. The S_{ML} values are percent saturation at the beginning of the run. 100% S_{ML} indicates a saturated solution. Percent saturation, S_{ML}, was computed using the Bechtel Modified Radian Equilibrium Program (BMREP). This computer routine, developed by Bechtel Corp. and Radian Corp. (Epstein, 1975), calculates solution equilibria for the components commonly found in FGD scrubber liquors. BMREP uses ionic concentrations in the feed solution as input variables. Output is in the form of solution equilibrium concentrations at saturation or percent saturation prior to crystal formation.

Conclusions

Based on the results of the metastability studies, it was found that the "Up and Down" technique is a rapid method for quantitatively comparing the combined effects of chemical additives on homogeneous nucleation and growth. The individual effects on nucleation and growth,

Table 1. Experimental Results of Chemical Additive Effects on Metastable Limit.[a]

Chemical Additive	Concentration (ppm)	Concentration (mM)	Metastable Limit, % Saturation, S_{ML}
Control	-	-	195
NMTP	30	0.1003	921
Citric acid	30	0.1428	294
Adipic acid	30	0.2053	272
	21	0.1428	185
Gelatin	30	-	256
Sodium oleate[b]	<30	<0.0987	239
EDTA	42	0.1428	226
SDBS[b]	<50	<0.1428	184
TCMAC[b]	70	0.1428	-

[a] For all experimental runs: Ca^{++} = 0.04466 M; Mg^{++} = 0.00823 M; K^{+} = 0.00281 M; Cl^{-} = 0.1086 M; temperature = 50°C; and initial pH = 5.5.

[b] These chemical additives formed precipitates when introduced to the $CaCl_2$ feed solution. All solids were filtered prior to metering to crystallizer.

however, cannot be separated using this method. Increased metastable limits, as defined in this experiment, may be the result of either decreased growth rates or delayed nucleation. If increased metastability was the result of delayed nucleation, it is still not possible to predict whether delayed nucleation in a batch process will equate to decreased nucleation rates in an MSMPR crystallizer. Thus, the "Up and Down" statistical method is probably not adequate for correlating effects of chemical additives to an MSMPR configuration. Its principal use would be that of scanning large classes of potential additives that

might be crystal modifiers, i.e., change crystal growth, nucleation, or habit.

An attempt to separate the additive effects on growth and nucleation was made during one experimental run by measuring solution conductivity changes as a function of time. It was thought that the time to nucleate would be evidenced by an abrupt decrease in solution conductivity. The result of this test was inconclusive. It was found that the conductivity (as measured with a portable ohm-meter) continually decreased with time. This may have been the result of plating on the electrodes in solution or some form of electrolytic catalysis of the crystallization process.

The results of Table 1 indicate that the greatest effect on metastability was produced by the addition of NMTP to the system. This compound has three phosphate functional groups associated with it. It is felt that this result is consistent with work performed by van Rosmalen (1981) with gypsum using HEDP, another phosphate, and McCall and Tadros (1979) on the calcium sulfite system using NMTP.

Work performed by McCall and Tadros (1979) on calcium sulfite also demonstrated that the greatest effects on metastability were caused by NMTP and citric acid. They also found the large effect produced by NMTP that this study has shown. They scanned four categories of chemical additives:

1. Low molecular weight carboxylic acids.
2. Proteinaceous materials.
3. Long-chain polymers with carboxy side chains.
4. Chelating agents.

It was expected that the degree of nucleation or growth inhibition caused by chemical additives with like functional groups would increase as the number of functional groups per molecule increased. To investigate this hypothesis, a comparison of adipic acid (2 -COOH groups), citric acid (3 -COOH groups), and EDTA (4 -COOH groups) was made. As can be seen in Table 1, the effect on metastability increases from adipic acid to citric acid. However, there is a decrease in the metastable limit for EDTA. This may be the result of stereo-chemical hindrance at the adsorption site due to the number of functional groups present. Also, tests run with EDTA were performed at a later date than those for the other chemical additives. Thus, changes in the minimum detectable crystal size would seriously affect any S_{ML} comparison with the remainder of the data of Table 1.

In general, this study was conducted with chemical additives found from the literature (van Rosmalen, 1981; Michaels et al., 1964; McCall and Tadros, 1979) to be effective in other crystallizing systems. Only two functional groups (-COOH and -POOH) were compared. Also, only anionic additives were tested. To determine the effects of cationic additives, an experimental attempt was made using TCMAC, a chloride. It was found that this compound was insoluble in the $CaCl_2$ feed solution so no results were obtained.

Crystallization Kinetics of $CaSO_3 \cdot 1/2H_2O$

Apparatus

Data for the generation of kinetic expressions (equations [2] and [5]) were obtained in an MSMPR crystallizer. For this purpose, the

PDI mini-nucleator was again used. The experimental setup was exactly the same as that for the metastability studies, only with continuous flow using the liquid level controller on the product removal port (see Figure 6).

Procedure

Prior to each experimental run the 2-liter feed flasks were filled with $NaHSO_3$ and $CaCl_2$ feed solutions. The $CaCl_2$ feed solution consisted of 2 liters containing: 27.46 gm $CaCl_2 \cdot 2H_2O$, 7.00 gm $MgCl_2 \cdot 6H_2O$, 0.88 gm KCl, and a chemical additive. The $CaCl_2$ feed flask was continually stirred throughout the experiment.

The $NaHSO_3$ feed flask was filled (under nitrogen purge) with 2 liters of aqueous solution containing a mole ratio of $NaHSO_3$:NaOH equal to 3.33:1.0. This gave a crystallizer inlet pH of approximately 5.5.

After filling the feed flasks, the mini-nucleator was filled with filtered distilled H_2O, connected to the sample stand, and allowed to heat up to 50°C. The impeller was turned on and set to about 650 RPM. The experiment began when the two feed pumps were simultaneously started. Supersaturation within the crystallizer was varied by 1) altering the inlet $SO_3^=$ ion concentration; and 2) running the experiment at different residence times, τ. The residence time was varied between 5 and 20 minutes for the 230-ml volume crystallizer.

The experiment was allowed to run for 5 residence times prior to data acquisition. Beginning at 5τ, CSD measurements were made every τ using the PDI-80xy. Measurements were taken until at least 3

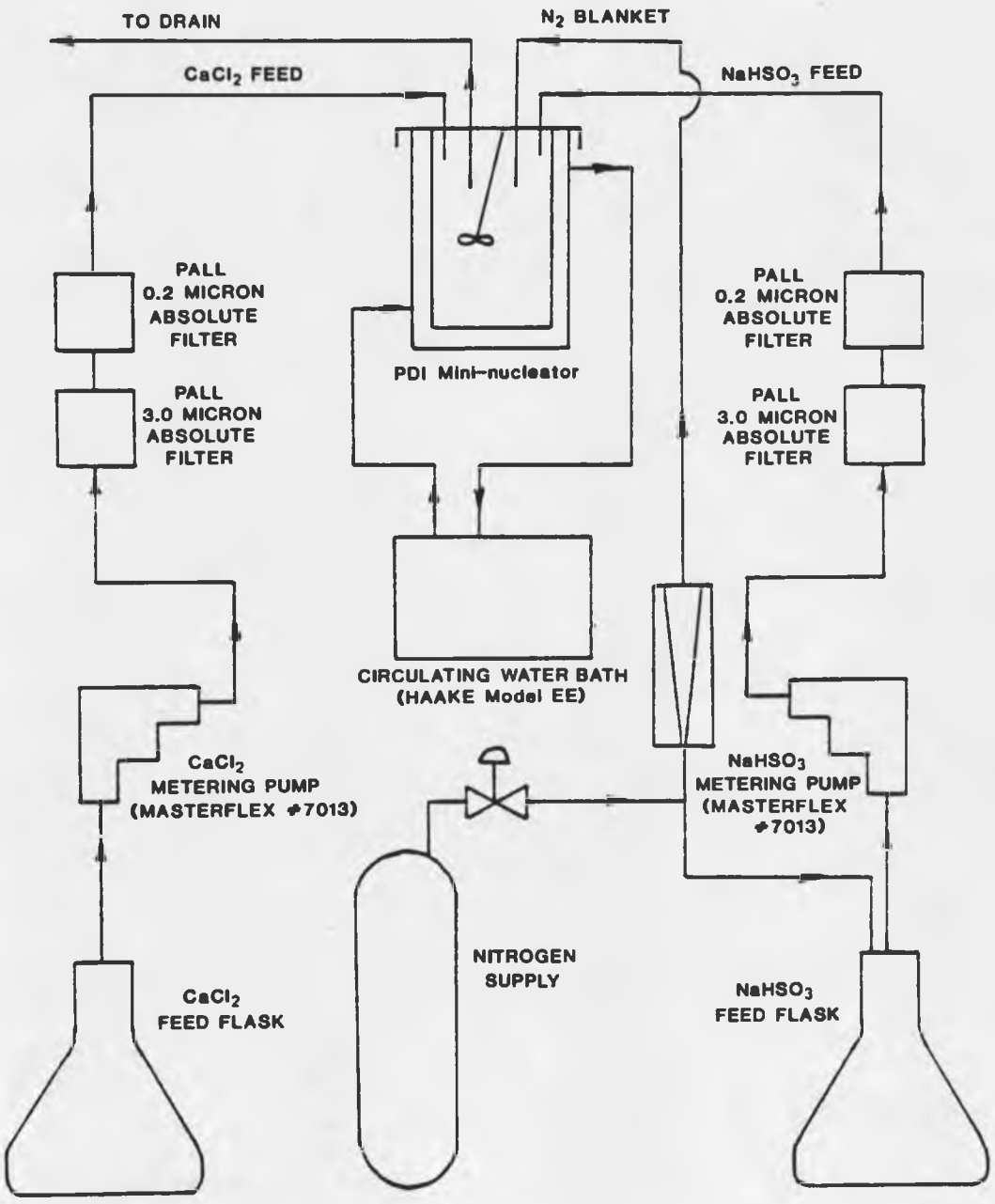

Figure 6. MSMPR Experimental Flow Diagram.

steady-state values were obtained. Steady state was defined as obtaining less than 5% difference in total number of counts (particles) in the 2-ml sample volume between measurements. It was also necessary to obtain consecutive growth rates within 10% of each other.

Although the PDI-80xy crystallization program determines the crystallizer slurry density, M_T (mg solid/liter clear liquor), it was found from past experience that this value may vary significantly even at steady state. For this reason, M_T measurements were made independently by removing a 20-ml syringe sample from the crystallizer and filtering through a 5-micron absolute Millipore filter. The solids were dried and weighed. The M_T calculated was then compared with the PDI generated M_T.

Additionally, since $CaSO_3 \cdot 1/2H_2O$ tends to form scale on the wall, a total solids sample was obtained at the end of each experimental run by filtering the total contents of the mini-nucleator through a Watman Qualitative 1 filter. This filter has an absolute rating of 11 microns. The M_T was subtracted from the total solids mass to determine the amount of scale accumulation throughout the run. This was then averaged over the run time to obtain a rate of deposition which was included in final M_T values.

MSMPR runs were conducted both with and without chemical additives. The chemical additives tested were NMTP and citric acid. Each set of experimental runs was made at four different residence times and three different inlet supersaturations. Crystal samples from each run were scanned with both an optical microscope and an SEM to compare

effects of the various chemical additives on crystal habit. The range of crystallizer inlet concentrations studied is shown in Table 2.

Results

Tables 3 and 4 are tabulations of results obtained during the MSMPR experiments. Table 3 lists results for blank (no chemical additive) runs. Table 4 shows results for the same configuration but with 30 ppm citric acid. For experiments conducted with 30 ppm NMTP, significant sustained nucleation was only possible for crystallizer inlet supersaturations above 1000% as calculated from BMREP. It was felt that this level of supersaturation was unrealistically high for a flue gas scrubber effluent liquor. Therefore, the experiments were terminated.

Table 2. Crystallizer Inlet Concentrations for MSMPR Experiments. -- pH = 5.5; temperature = 50°C.

	Concentration		
Ion	(ppm)	(mM)	Source
Ca^{++}	1790	44.66	$CaCl_2 \cdot 2H_2O$
Mg^{++}	200	8.23	$MgCl_2 \cdot 6H_2O$
K^{+}	110	2.81	KCl
Cl^{-}	3850	108.60	(above)
Na^{+}	1240-871	54.12-57.89	NaOH, $NaHSO_3$
$SO_3^{=}$	3333-2333	41.63-29.14	$NaHSO_3$

Table 3. MSMPR Results with No Modifier.

Run No.	Residence Time, τ (min)	Inlet Supersaturation (mg/l $CaSO_3 \cdot 1/2H_2O$)	M_T[a] (mg/l)	B^o[b] (#/cc-min)	G[c] (μm/min)	$\bar{L}_{1,0}$ Population Average Size, $G\tau$ (μm)	$\bar{L}_{4,3}$ Mass Average Size (μm)
17	20	1394	-	-	0.746	14.92	59.7
18	15		-	-	1.010	15.15	60.6
19	15		919	2766	0.938	14.07	56.3
20	20		1324	2233	0.775	15.50	62.0
21	20	1237	1162	2775	0.690	13.80	55.2
22	15		1151	3166	0.966	14.49	58.0
23	10		1137	3860	1.547	15.47	61.4
24	15	911	892	2440	0.965	14.52	58.1
25	10		849	4148	1.370	13.70	54.8
26	5		913	8816	2.750	13.75	55.0
Average						14.50	58.0

[a] Determined from 20-ml slurry sample.

[b] Calculated from mass balance equation.

[c] Obtained from PDI-80xy output.

Table 4. MSMPR Results with 30 ppm Citric Acid.

Run No.	Residence Time, τ (min)	Inlet Supersaturation (mg/l $CaSO_3 \cdot 1/2H_2O$)	M_T[a] (mg/l)	B^o[b] (#/cc-min)	G[c] (μm/min)	$\bar{L}_{1,0}$ Population Average Size, $G\tau$ (μm)	$\bar{L}_{4,3}$ Mass Average Size (μm)
31	15	1394	1552	13636	0.656	9.84	39.4
32	20		1511	13921	0.440	8.80	35.2
33	10		1467	31079	0.840	8.40	33.6
34	15	1237	-	-	0.698	10.47	41.9
35	20		1358	6512	0.547	10.94	43.8
36	10		1079	30864	0.760	7.60	30.4
37	10	911	897	18207	0.852	8.52	34.1
38	5		900	34756	1.733	8.67	34.7
39	15		1102	13309	0.590	8.85	35.4
Average						9.12	36.5

[a] Determined from 20-ml slurry sample.

[b] Calculated from mass balance equation.

[c] Obtained from PDI-80xy output.

Slurry densities, M_T, were determined from filtered 20-ml slurry samples taken during the experimental runs. The M_T's were generally found to be equal to the inlet supersaturation calculated from BMREP. This indicates that the $CaSO_3 \cdot 1/2H_2O$ system is Class II (operating at essentially zero residual supersaturation). Measured slurry densities greater than the inlet supersaturation are the result of inaccuracies of handling a small dilute sample. Additionally, any dislodged scale removed with the slurry sample produced a greater apparent M_T.

Due to the large number of particles (10,000-15,000 in a 2-ml sample) in a crystallizing system, the coincidence loss associated with the PDI probe could be as high as 30-50%. The correction made by the PDI-80xy was not accurate enough to use computed values of B^o, n^o, and M_T. These values are derived from the intercept of the cumulative number plot. Since errors in coincidence correction will not affect the slope, values of G were recorded directly from the computer output. Values of B^o were back-calculated from the measured values of slurry density using the mass balance equation:

$$M_T = 6\rho k_v B^o G^3 \tau^4 \qquad [13]$$

where k_v = shape factor = $\pi/6$.

Figure 7 graphically illustrates the effect of residence time, inlet superaturation, and citric acid concentration on population average size. The figure shows a population average size which appears to be invariant with both residence time and inlet supersaturation for the range of those variables tested.

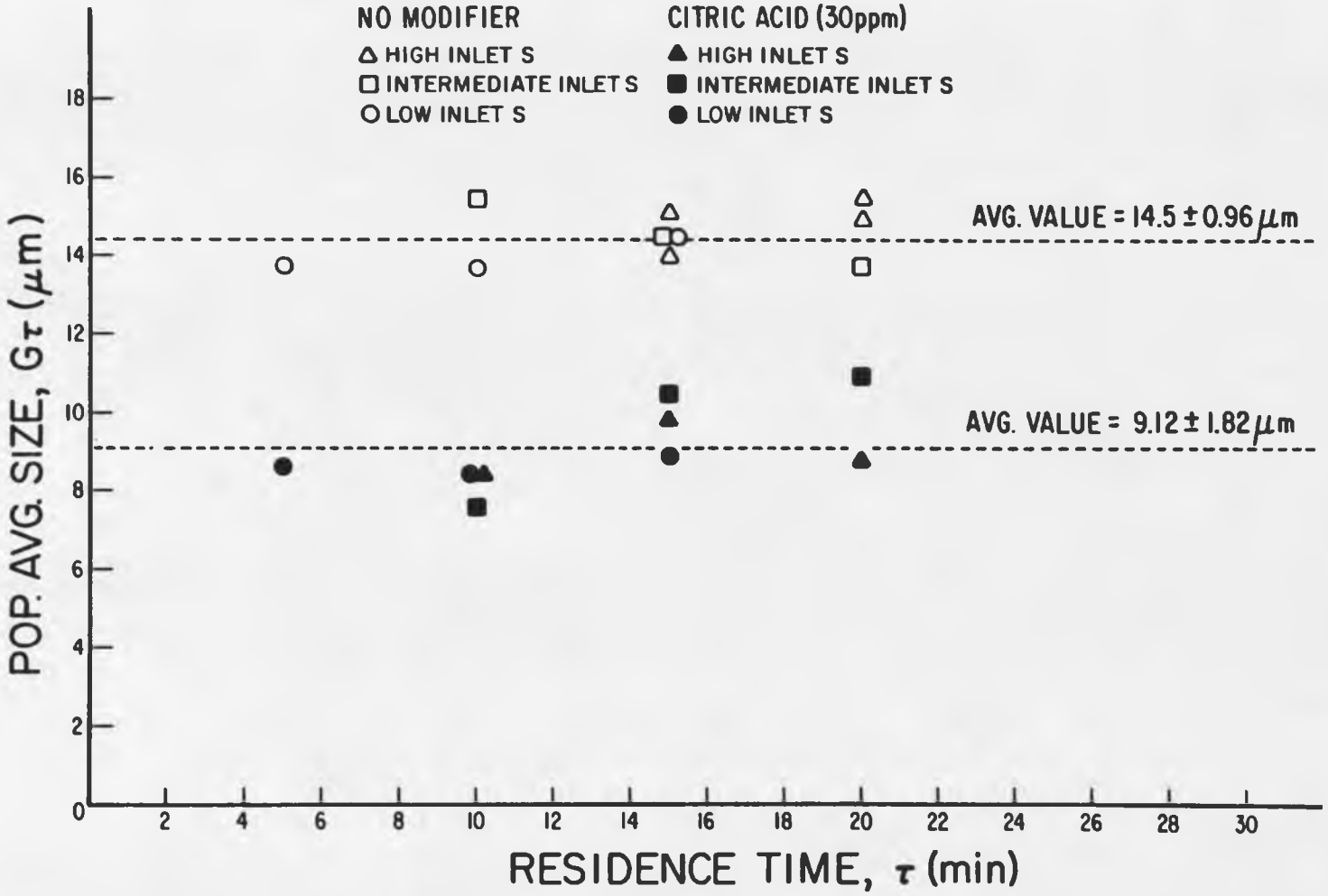

Figure 7. Population Average Size for the Mini-Nucleator.

The values from Tables 3 and 4 were fit to the nucleation power law, equation [2], with a multi-variable linear regression routine. The results of this fit are shown in Figures 8 and 9 for the control and citric acid data, respectively. The increased data scatter for the citric acid experiments is believed to be the result of variations in citric acid concentration. Figure 9 also shows that two points generated in work performed with a 9-liter crystallizer at the same time these experiments were conducted fall within the ±30% error bounds.

Due to the extremely small amount of residual supersaturation present in a Class II crystallizer, no supersaturation measurements were possible. Thus, the growth rate power law, equation [5], could not be fitted. Table 5 shows the results of the nucleation power law kinetics.

Photomicrographs and SEM photographs were taken at the end of each experimental run to compare crystal morphologies in the presence of the different chemical additives. Figure 10 shows photomicrographs of crystals obtained with no additive, citric acid, and NMTP, respectively. Figure 11 shows SEM photographs of crystals grown under similar conditions. From the photographs, it can be seen that both citric acid and NMTP yield a polycrystalline particle, while calcium sulfite grown in the absence of additive forms individual or loosely bound platelets.

Figure 12 shows the relative effects of precipitation rate on crystal habit for runs with no additive. Figure 13 is a similar display for crystals formed in the presence of citric acid. It can be seen that, for the ranges studied, precipitation rate had little effect on crystal habit. However, complex crystal habit as shown in Figure 13 is usually the result of rapid growth and/or high driving forces. No

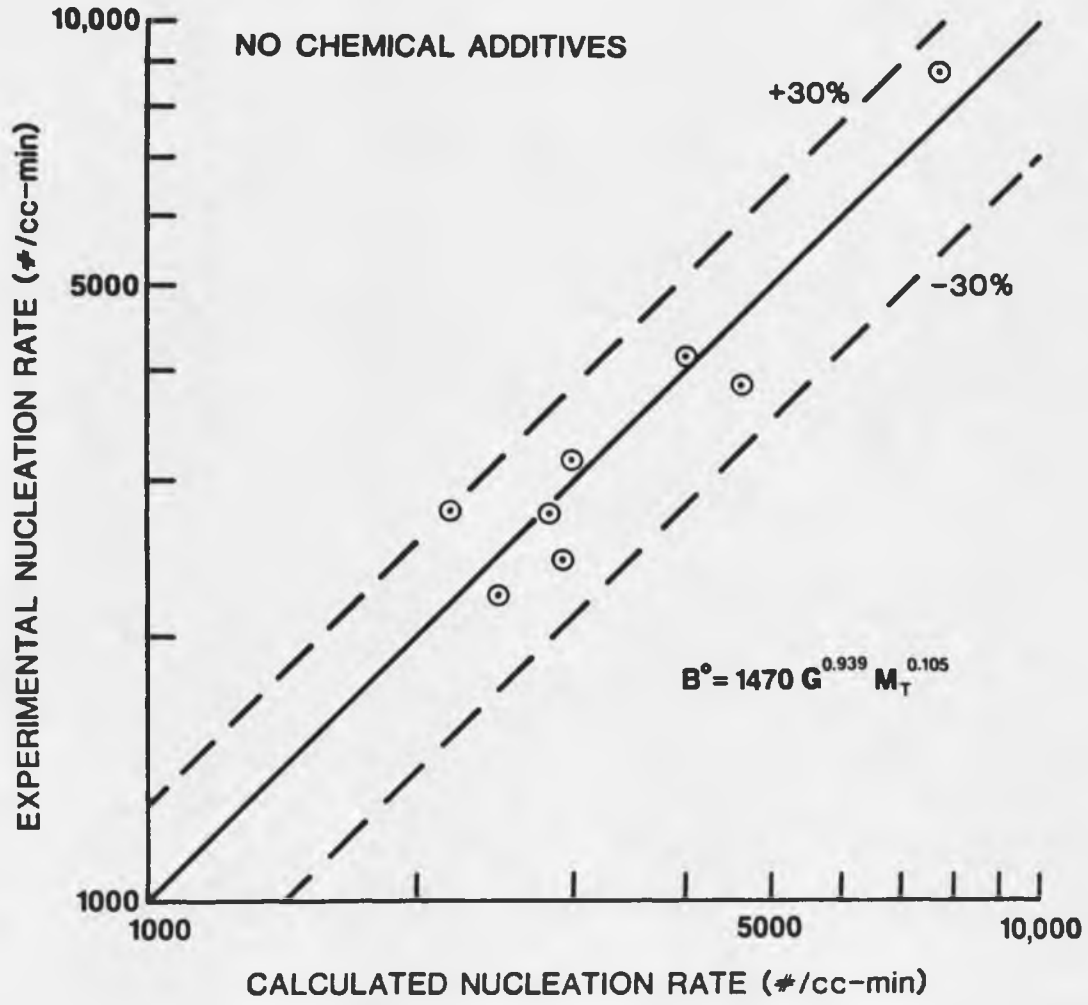

Figure 8. Power Law Correlation for Mini-Nucleator Data (Control).

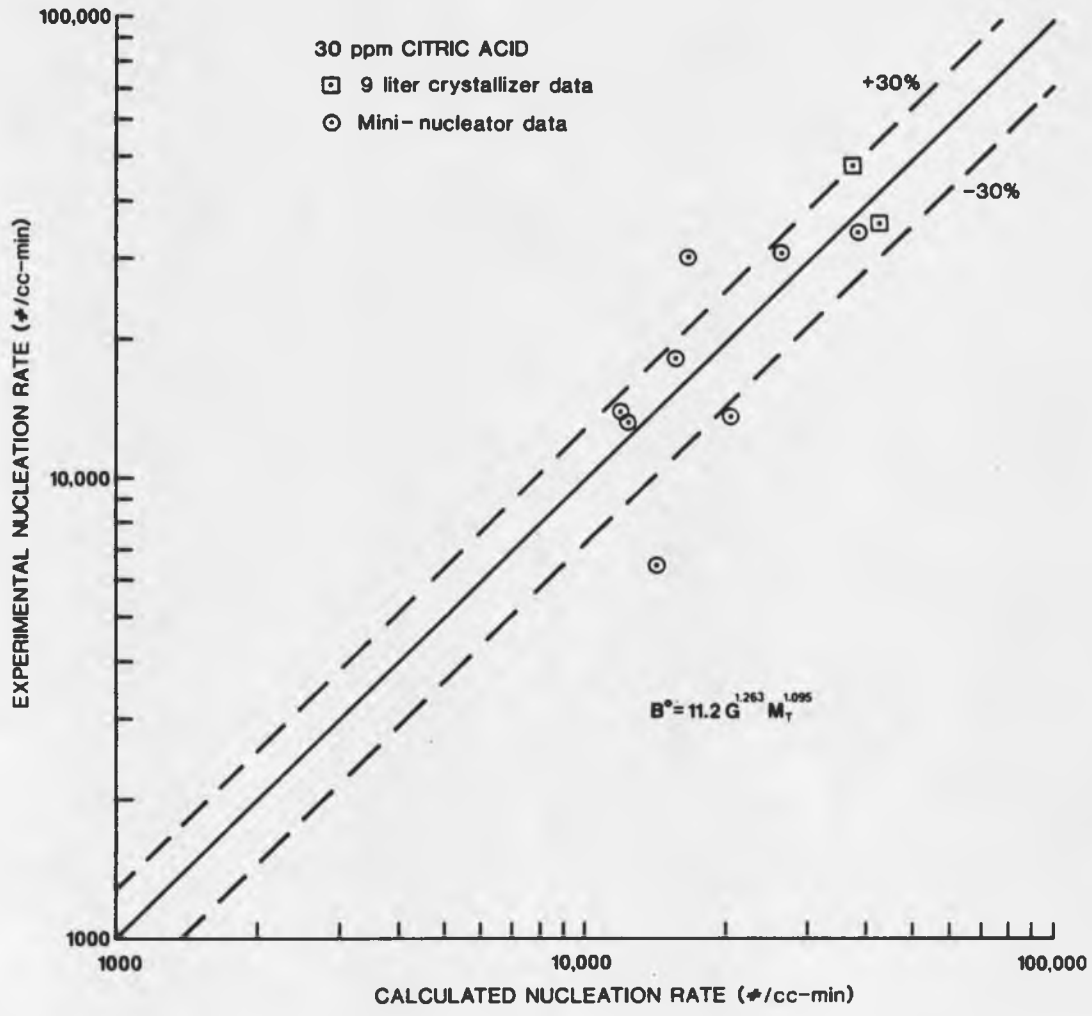

Figure 9. Power Law Correlation for Mini-Nucleator Data (30 ppm Citric Acid).

Table 5. Kinetic Parameters for $B^o = k_N M_T^j G^i$. -- B^o = #/cc-min; M_T = mg/l; and G = μm/min.

Experimental Conditions	k_N	j	i	r^2
Control (no additive)	1470.	0.105	0.939	0.885
30 ppm Citric acid	11.16	1.095	1.263	0.619

method of comparing the effects of residual supersaturation was possible due to the unmeasurable amount present in a Class II crystallizer. Therefore, the actual driving force for growth was probably approximately constant for all samples.

Clearly, in these experiments, the platelet is the predominant crystal habit for $CaSO_3 \cdot 1/2H_2O$ grown in the absence of chemical additives. Both NMTP and citric acid tend to cause the formation of polycrystalline particles, with citric acid producing a more spiny crystal and NMTP creating groups of discs. Platelets have been reported previously (Edwards, 1979; Crowe and Seale, 1979; McCall and Tadros, 1979) as the result of systems initially seeded with platelets or as the result of precipitation with a limestone calcium source. In these experiments, there was neither seeding nor the use of limestone. Although not found in this study, calcium sulfite with spheroidal habit has been seen during work performed by other experimenters (Crowe and Seale, 1979; McCall and Tadros, 1979). McCall and Tadros (1979) obtained spherical particles during tests with citric acid in a limestone system.

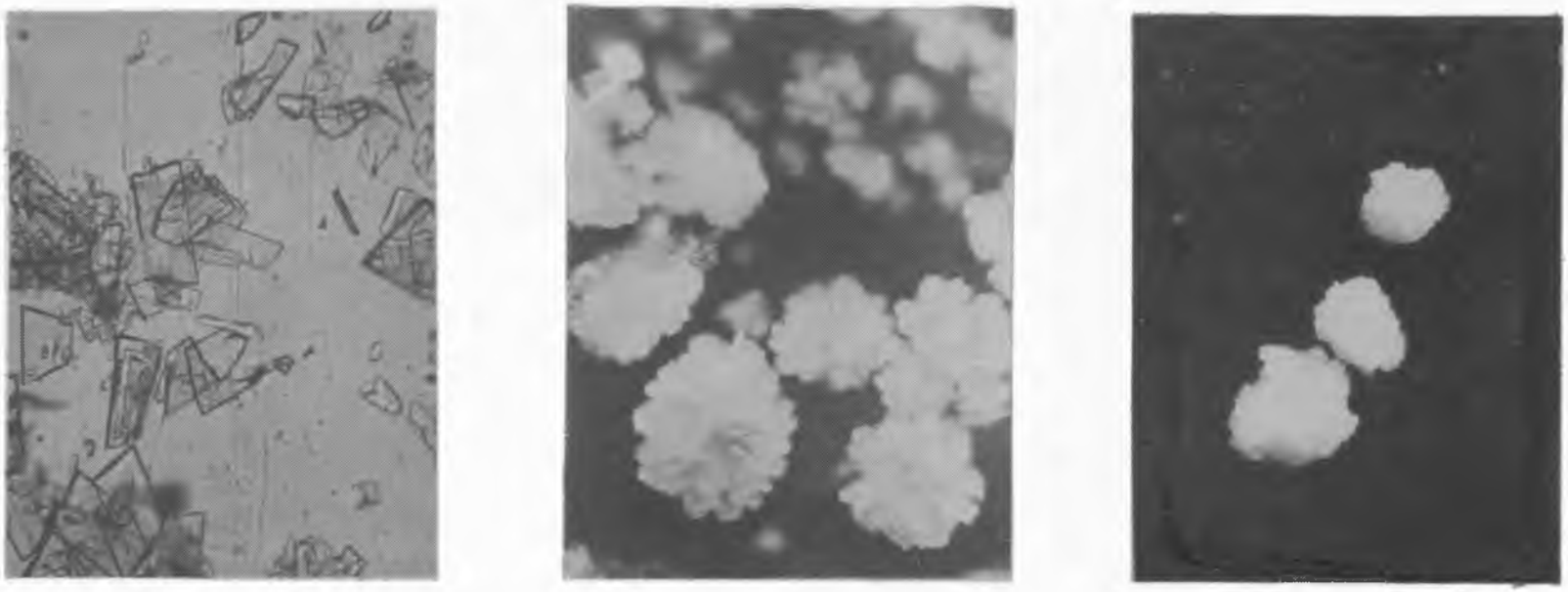

(a) (b) (c)

Figure 10. Photomicrographs of Mini-Nucleator Product. -- (a) No additive, 20X; (b) 30 ppm citric acid, 10X; (c) 30 ppm NMTP, 4X.

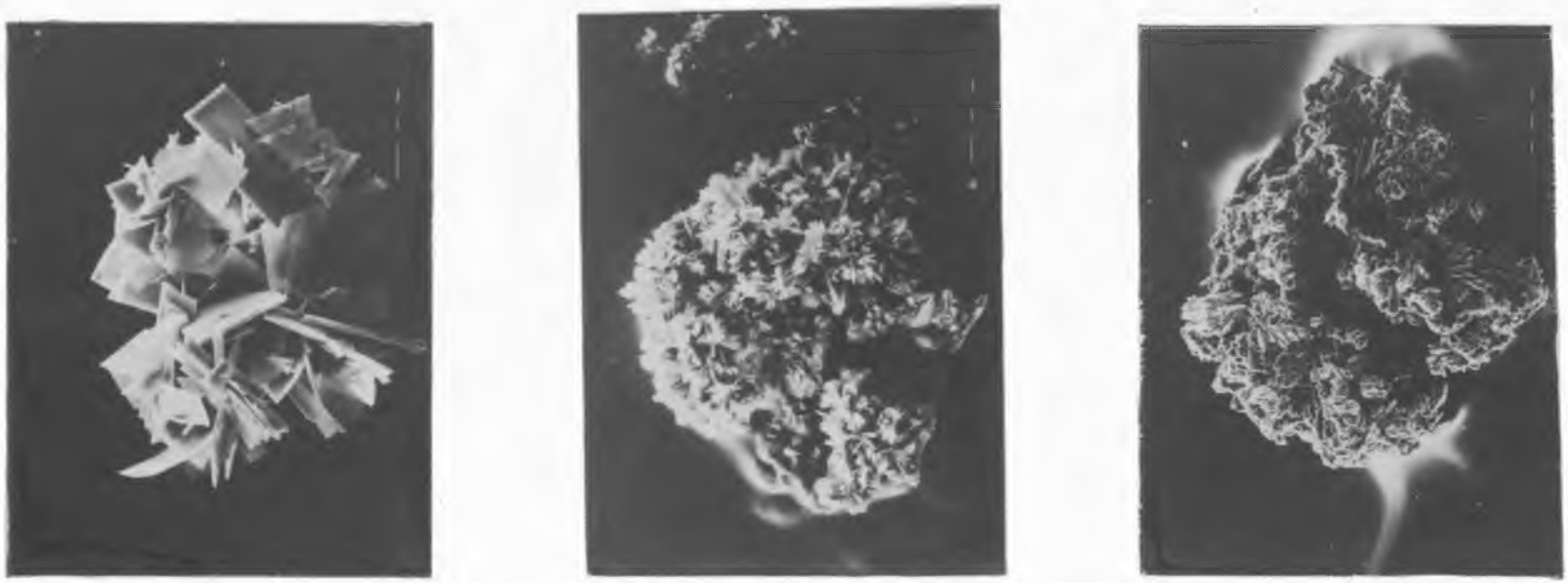

(a) (b) (c)

Figure 11. SEM Photographs of Mini-Nucleator Product. -- (a) No additive, 630X; (b) 30 ppm citric acid, 500X; (c) 30 ppm NMTP, 180X.

(a)

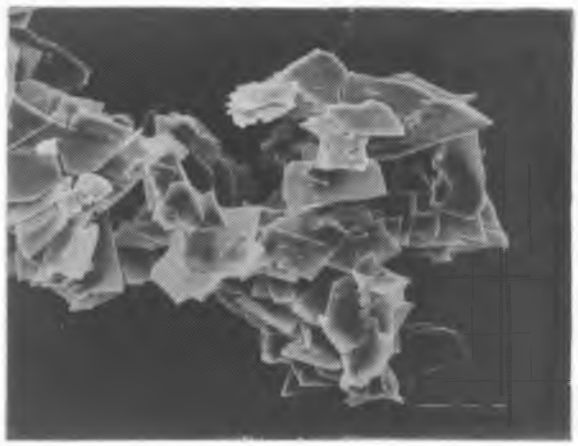

(b)

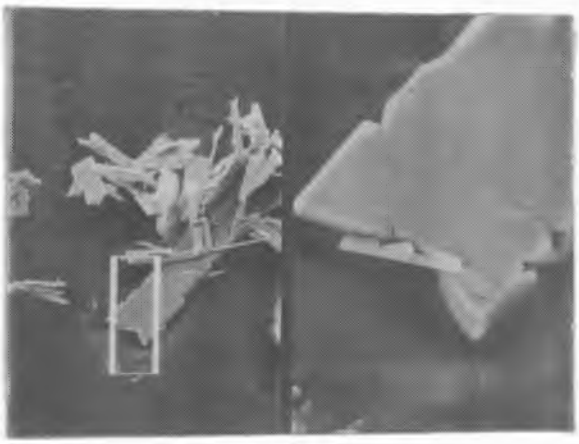

Figure 12. Effect of Precipitation Rate on Morphology of $CaSO_3 \cdot 1/2H_2O$ (Blank). -- (a) Precipitation rate = 182.2 mg/l-min, 400X; (b) precipitation rate = 61.9 mg/l-min, 300/3500X.

(a) (b) (c)

Figure 13. Effect of Precipitation Rate on Morphology of $CaSO_3 \cdot 1/2H_2O$ (30 ppm Citric Acid). -- (a) Precipitation rate = 139.4 mg/l-min, 1000/5000X; (b) precipitation rate = 123.7 mg/l-min, 1300X; (c) precipitation rate = 61.9 mg/l-min, 450/2250X.

Conclusions

Throughout these experiments, it was found that in-line CSD measurement with the PDI-80xy was insufficiently accurate for determination of crystallization parameters other than growth rate. Due to the relatively large numbers and sizes of particles involved in crystallization processes, in-line detection with no sample dilution results in 30-50% coincidence loss. Corrections for this coincidence loss are not accurate enough to enable use of numbers generated from intercept values of the cumulative number plot. Values of growth rate obtained from the slope of the cumulative plot were regarded as correct since coincidence correction is a fractional correction applied to all data channels and, hence, does not alter the slope.

Experiments conducted with calcium sulfite in a 9-liter crystallizer at The University of Arizona gave good agreement with mini-nucleator data for population average size when using citric acid. However, population average size with no chemical additive was about 8 microns in the 9-liter crystallizer but 14.5 microns in the mini-nucleator. Both systems continued to show Class II behavior. A series of tests was run on the mini-nucleator to determine if agglomeration was a factor. Twelve 4-mm glass beads were placed in the mini-nucleator to act as deagglomeraters. In the presence of the glass beads, the population average size decreased from 14.5 microns to approximately 8-9 microns with no chemical additive. With 30 ppm citric acid present, the glass beads had no effect on crystal average size. The results indicate that agglomeration may be a factor in the runs with no chemical additive. However, the results were not entirely conclusive since poor exponential

distributions were obtained when the beads were used with no additive present, possibly indicating breakage as well as deagglomeration.

Assuming agglomeration is not a factor in the unmodified mini-nucleator runs, the results show that citric acid acts to decrease growth and enhance nucleation. This was predicted from the metastable limit studies where it was hypothesized that $t_g > t_n$. Also, the results indicate that $CaSO_3 \cdot 1/2H_2O$ is a Class II crystallizing system and nucleation rate has an approximate first-order dependence on growth rate for both the control and citric acid modified systems. However, nucleation rate showed only a small dependence on slurry density for the control runs while having a first-order dependence in the presence of citric acid. This may be the result of the drastically different crystal habits. Crystal-crystal contact in the citric acid modified system (multi-faceted polyhedral crystal structure) would probably generate more nuclei than the same level of contact in a pure system where only individual platelets are found.

Citric acid and NMTP produced significant effects on the overall morphology of $CaSO_3 \cdot 1/2H_2O$. Citric acid created particles with a 25% smaller average size than those in the control runs. The crystals formed were needle-like polycrystalline particles. It is felt that such habit would not improve settling characteristics. The presence of NMTP resulted in a highly metastable system. The crystals produced were larger and had a much chunkier habit than the control runs. McCall and Tadros (1979) have reported similar results for NMTP. Additionally, they found that calcium sulfite precipitated in the presence of NMTP resulted in a slurry which settled 3-5 times faster, produced a settled

solids density 1.2-2 times greater, and a filter cake with an approximate 90% solids fraction. They also indicate that calcium sulfite precipitated in the presence of NMTP crystallizes as $CaSO_3 \cdot 4H_2O$.

CHAPTER 4

CRYSTALLIZER SIMULATION

The calcium sulfite crystallization kinetics generated in Chapter 3 can be used in various crystallizer simulation programs (Nuttal, 1971; Sibert, 1982) to study the effects of different process configurations on CSD. For the purposes of this simulation, the design basis scrubber precipitator used was that of the TVA Shawnee Test Facility (Epstein et al., 1973; Epstein, 1975).

Simulation

A simplified schematic of the TVA Test Facility is shown in Figure 14a. Due to the high scrubber recycle rate, the scrubber and hold tank can be considered as one vessel. Based on the TVA facility, this vessel has an approximate volume of 20,000 gallons and operates with a production rate of 6 tons/day. The discharge rate to the clarifier is approximately 20 gpm. Solids concentration in the clarifier bottoms varies to a maximum of 40 weight percent. The maximum particle size in the clarifier overflow was previously determined to be 10-15 microns (Etherton, 1980). The actual simulated configuration is shown in Figure 14b.

Due to the uncertainties of agglomeration in the MSMPR control experiments, kinetic data for the citric acid system was used for the simulation. These data combined with the above system parameters were

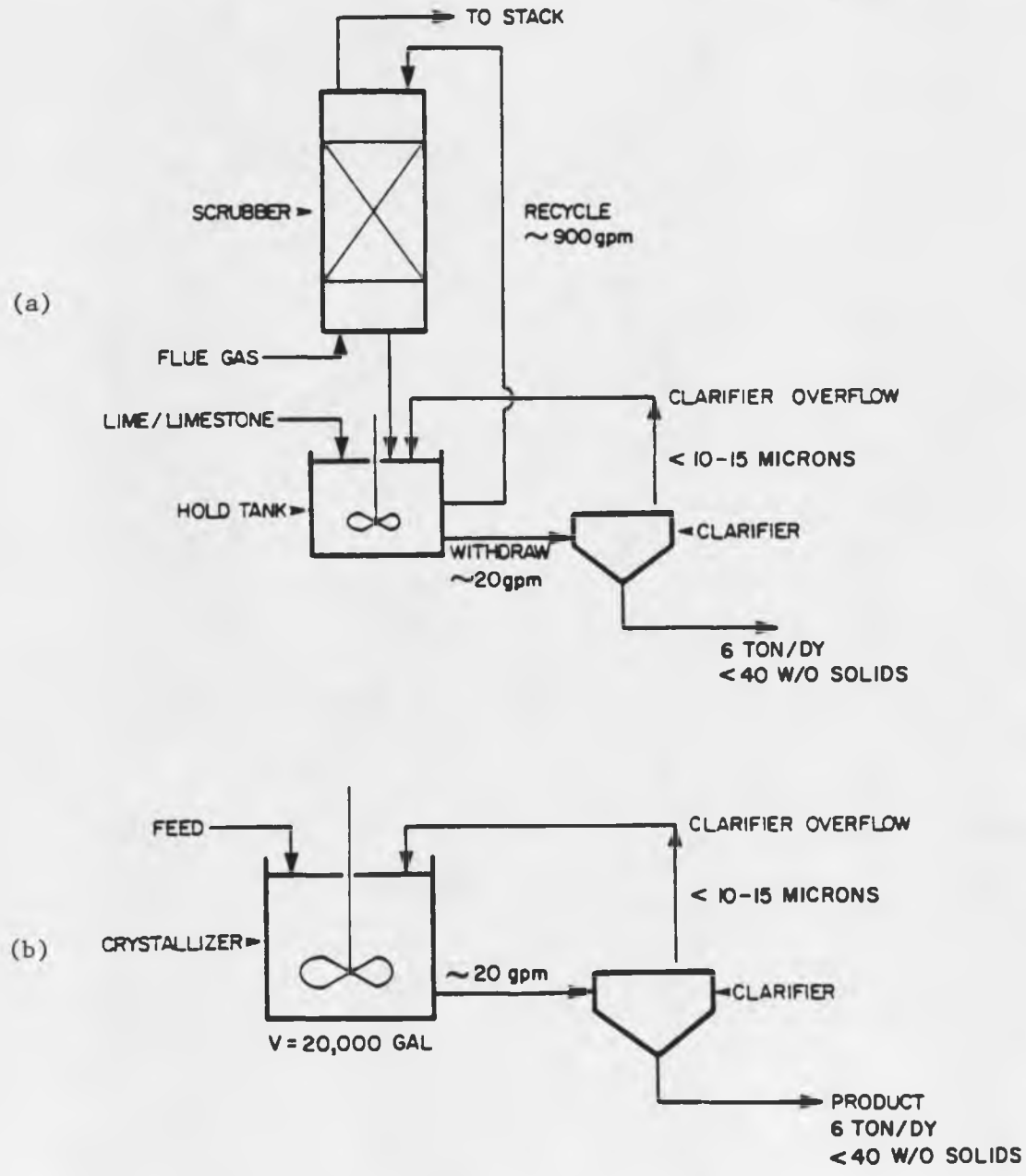

Figure 14. Scrubber Configurations. -- (a) Simplified schematic of TVA Test Facility; (b) actual simulated configuration.

used in the Mark I Crystallizer Simulator (Nuttall, 1971) for a steady-state Class II crystallizing system. The Mark I Simulator was used to predict both seed bed (hold tank) and product CSD for a scrubber precipitator with and without classified product removal. Classified product removal is the selective removal of various particle sizes from the crystallizer at different rates.

Three simulation cases were studied: 1) MSMPR, 2) present design, and 3) proposed design with classified product removal. The MSMPR is simply the base case of a mixed tank with no clarifier. The present design is a mixed tank employing a clarifier discharge and recycle. Various recycle ratios (ratio of clarifier overflow to underflow) were modeled. The proposed design consists of Double Draw-Off (DDO) streams from the crystallizer going to the existing clarifier. The objective of a DDO configuration is to remove small particles at a greater rate than the large ones. The proposed design was simulated at various DDO cut sizes, L_0, and DDO ratios (ratio of clarifier feed to DDO underflow). The three crystallizer configurations and particle removal functions are shown in Figure 15. Recycle ratios were varied between 4 and 14. DDO ratios were varied between 3 and 5 with classification at 30, 50, and 70 microns. The effect of reduced clarifier cut size was also modeled between 5 and 15 microns.

Results

Results of the scrubber simulation are shown in Figures 16, 17, and 18. Figure 16 shows results obtained by varying the recycle ratio from the clarifier with no DDO. The results are for a clarifier cut

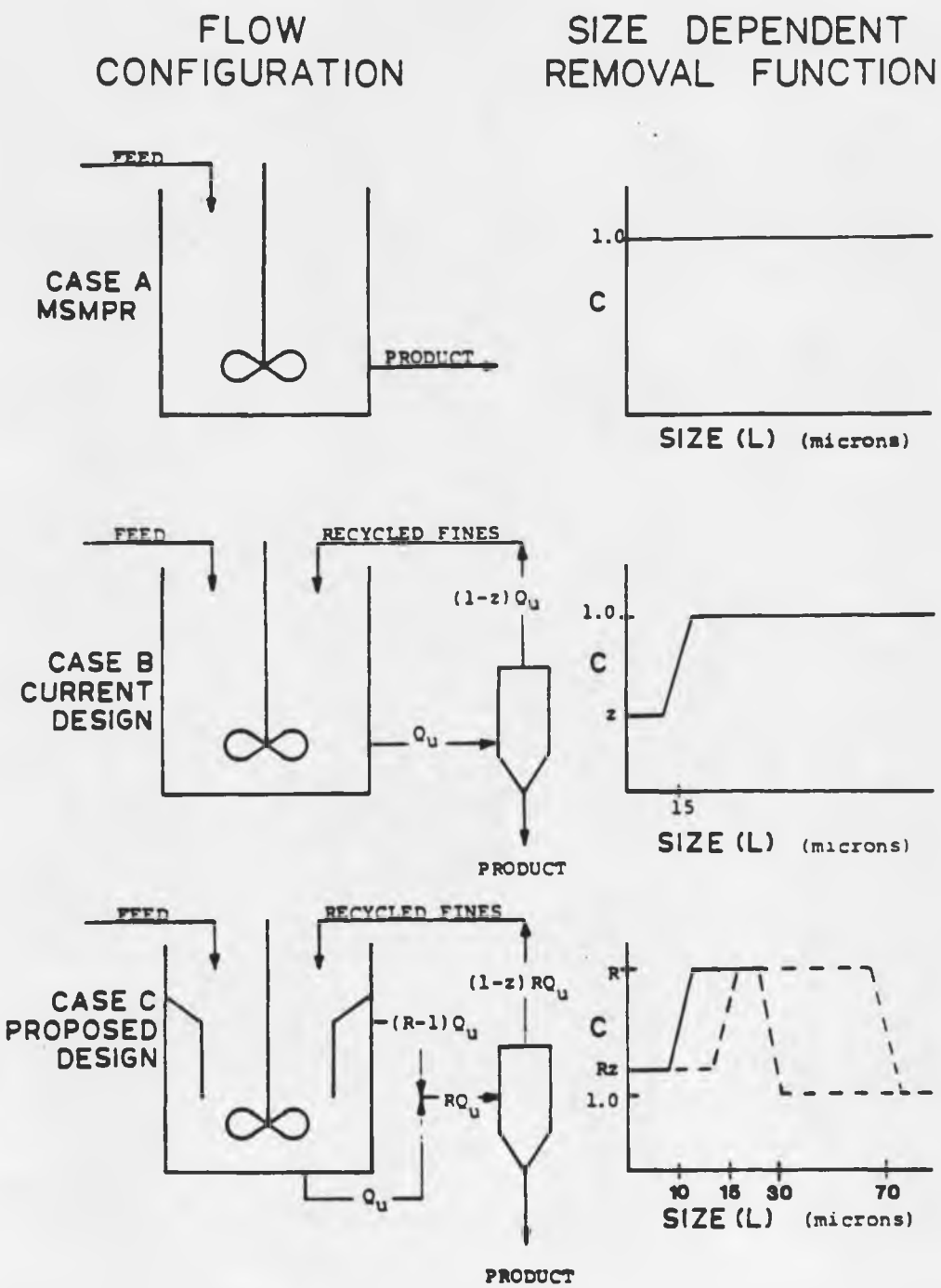

Figure 15. Simulated Scrubber Configurations.

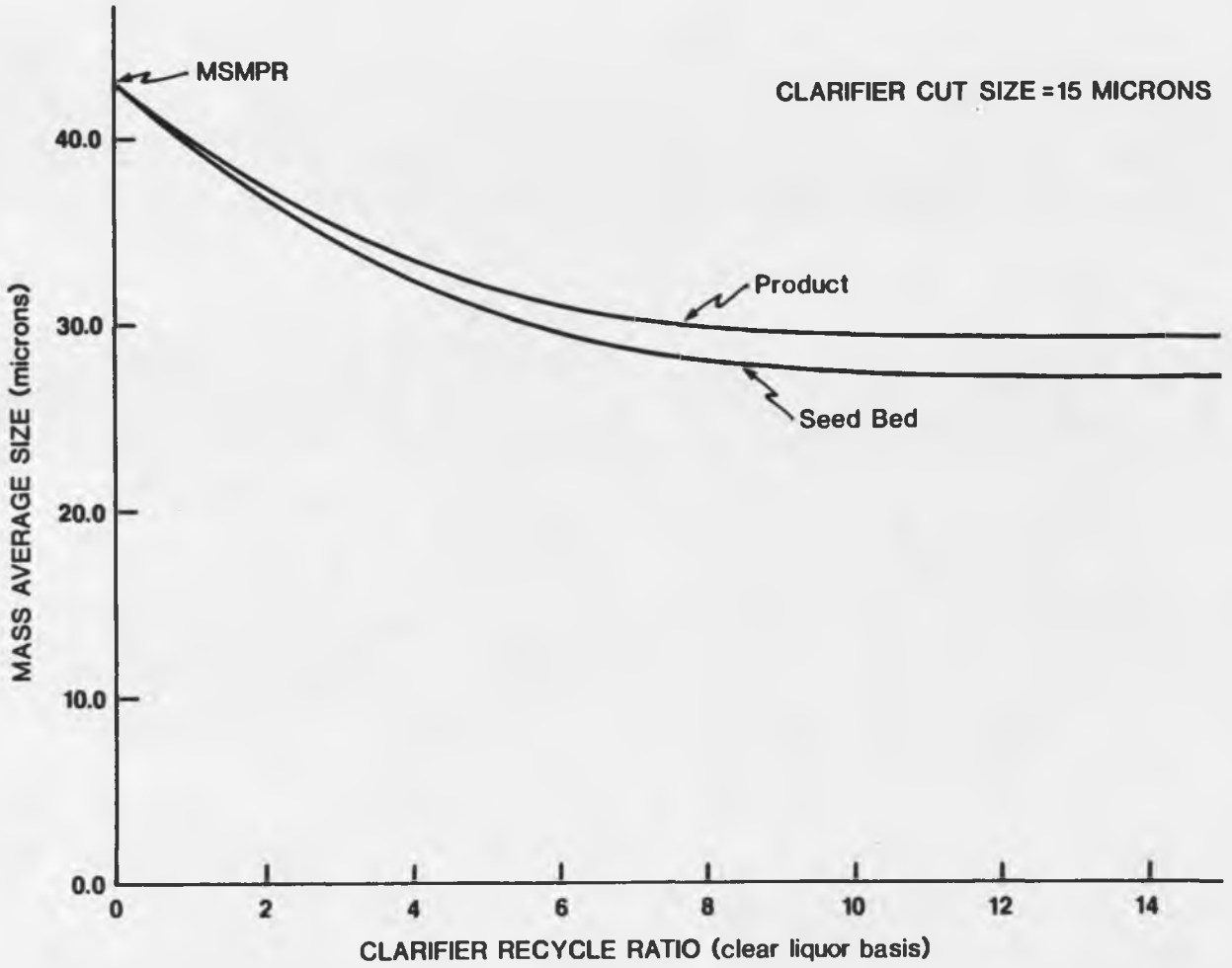

Figure 16. Effect of Recycle Ratio on Product and Seed Bed Mass-Average Size.

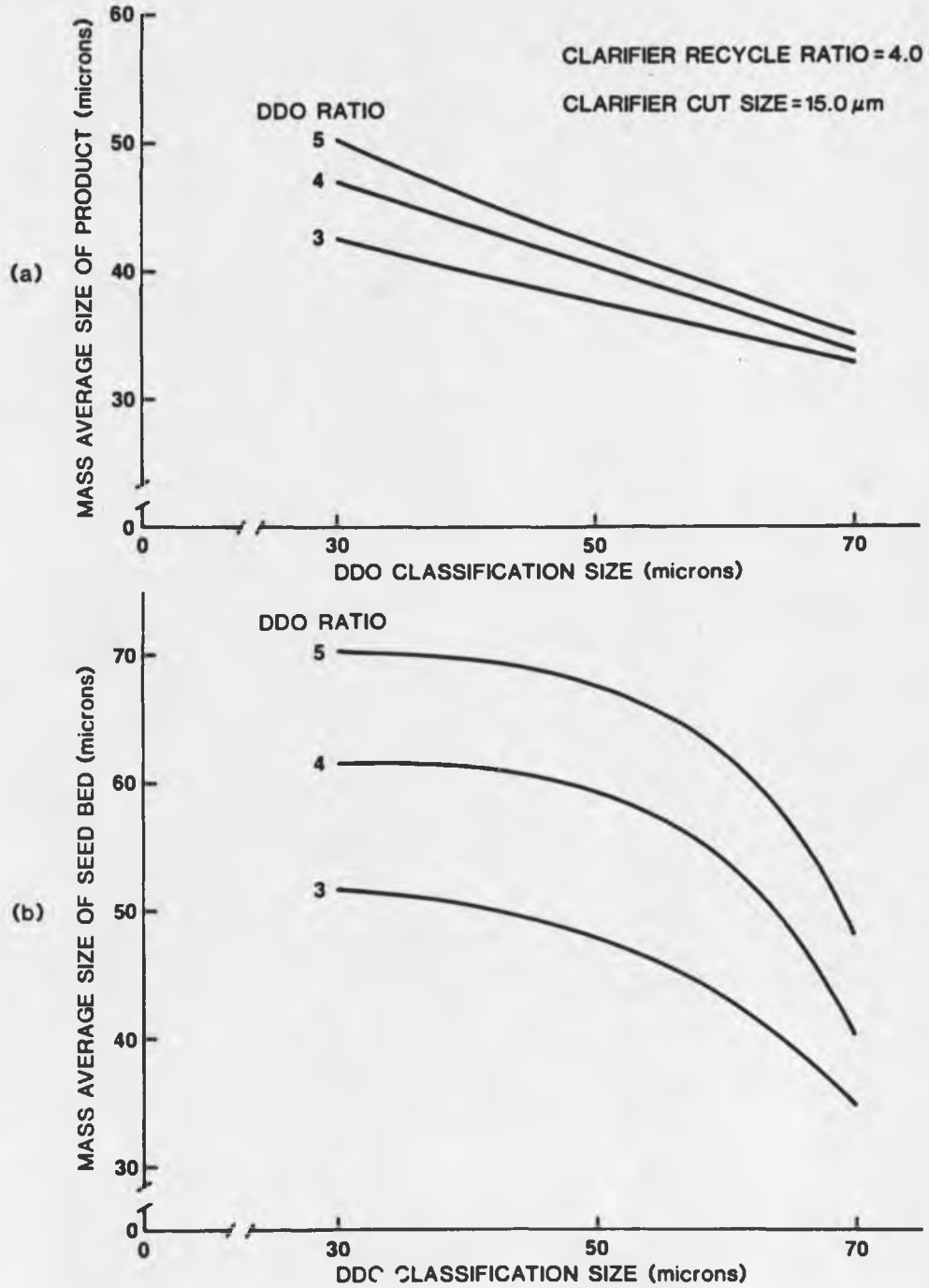

Figure 17. Effect of DDO Ratio and Classification Size on Mass-Average Size of Product (a) and Seed Bed (b).

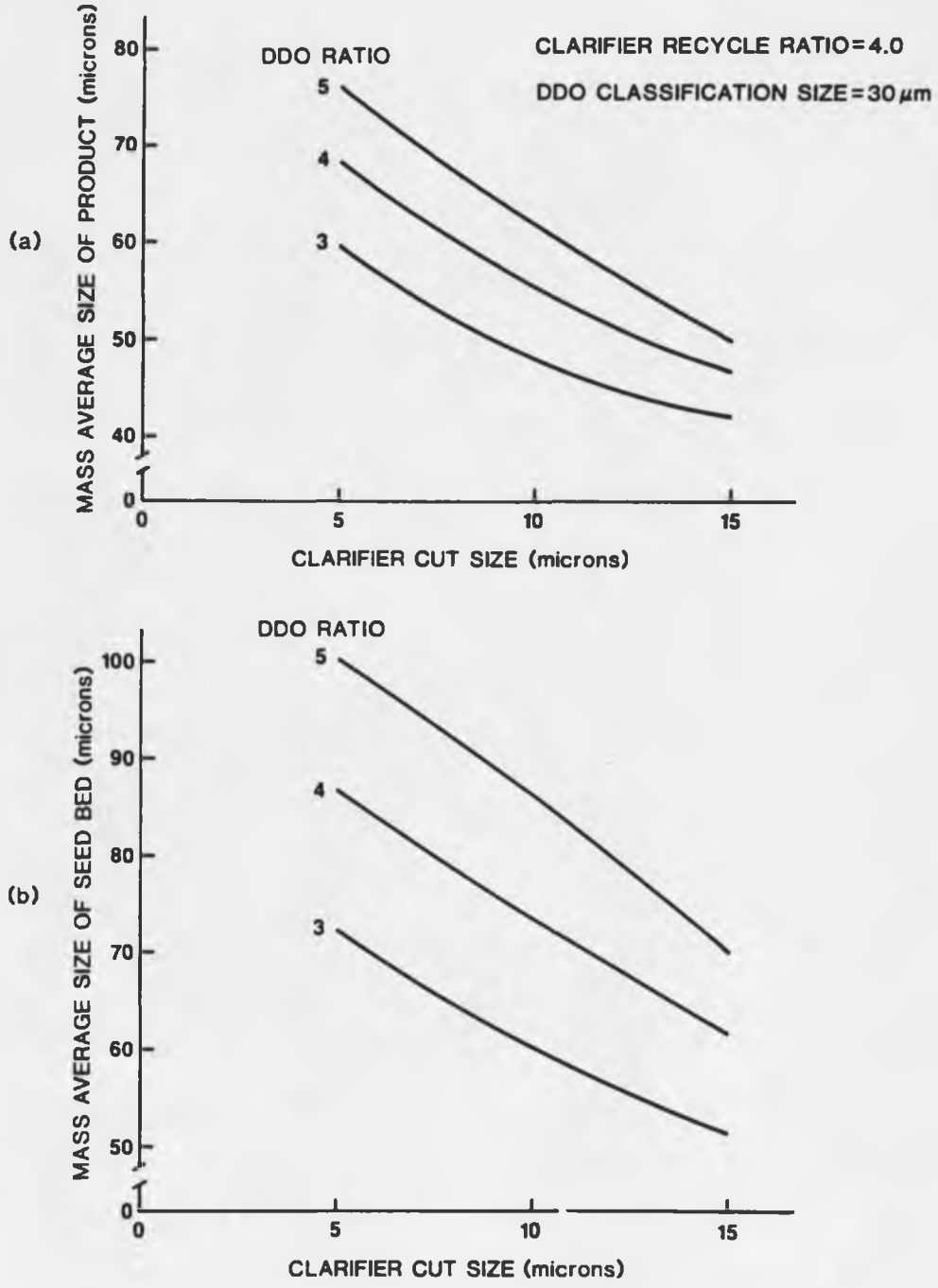

Figure 18. Effect of DDO Ratio and Clarifier Cut Size on Mass-Average Size of Product (a) and Seed Bed (b).

size of 15 microns in the recycle stream. It can be seen that a low recycle ratio yields a greater product mass-average size. However, the trade-off is for a smaller product solids density with decreased recycle. Table 6 shows the effect of recycle ratio on product solids density.

Figure 17 shows the effect of DDO ratio and hold-tank classification size on crystal mass-average size. A classification size of 70 microns results in product and seed bed average sizes approaching those of the present design, at a recycle ratio of 4.0. Decreasing the hold-tank classification size results in a larger fraction of the product crystals being removed with a longer residence time. This results in a greater mass-average size in the hold tank and the product stream.

Figure 18 shows the effect of improved clarification prior to recycle of the clarifier overflow. Significant increases in product average size were found by decreasing the clarifier cut size from 15 to 5 microns at a fixed DDO ratio and classification rate.

Table 6. Product Solids Fraction as a Function of Clarifier Recycle Ratio.

Recycle Ratio	Weight Percent Solids in Product Stream
14.0	43
9.0	33
5.67	25
4.0	20

Conclusions

From the standpoint of product average size, the present scrubber design is the least efficient. This is due to recycle of fines from the clarifier. Although clarifier recycle must be used to maintain scrubber liquor balances and partially dewater product, improved product size can be accomplished by both using a DDO configuration and decreasing the clarifier cut size. For a DDO ratio of 5 and classification at 30 microns, product mass-average size can be increased by a factor of 1.5 above that for the present design. Decreasing the clarifier cut size from 15 to 5 microns at a DDO ratio of 5 and classification at 30 microns will increase the product size by a factor of 2.3.

Etherton (1980) has reported that optimum design for a similar gypsum system occurs at a DDO ratio of 7 and a classification size of 50 microns. Although a DDO ratio of 7 was not modeled in this study, it appears from Figure 17 that increasing the DDO ratio to 7 would further increase product mass-average size. Etherton (1980) did not model the effect of variations in clarifier cut size.

Improved product mass-average size from scrubber liquors should result from a DDO hold-tank configuration and improved clarifier design. Improved flocculation techniques or filtration of clarifier overflow would reduce recycle of fines and might increase product size.

Etherton (1980) has suggested that by increasing the seed bed mass-average size the total available area for crystal growth will be decreased and, hence, increased fouling might occur. For a gypsum system, fouling is a greater concern than for a calcium sulfite system.

Gypsum is much harder than $CaSO_3 \cdot 1/2H_2O$ and, thus, can require mechanical methods for removal of scale. Calcium sulfite scale removal can be readily accomplished by low pH solution washing.

CHAPTER 5

CONCLUSIONS

1. Metastability of the calcium sulfite system can be measured by an "Up and Down" statistical technique. However, this technique cannot describe the individual effects of chemical additives on growth and nucleation.
2. Of the chemical additives scanned in this study, the greatest effects on metastability of calcium sulfite were produced by NMTP and citric acid.
3. NMTP and citric acid alter the characteristic platelet habit of $CaSO_3 \cdot 1/2H_2O$ to polycrystalline conglomerates. The presence of NMTP results in a more dense particle than citric acid.
4. The calcium sulfite system is a Class II crystallizing system, operating with negligible residual supersaturation.
5. Results of the MSMPR experiments carried out in the 240-ml mini-nucleator using citric acid as a chemical additive agreed with those generated with a 9-liter crystallizer. Experiments with no additive gave product average sizes which were 25% larger than those obtained from the 9-liter crystallizer. This may be due to agglomeration within the mini-nucleator, possibly the result of lower impeller energy input. Crystal size differences between the 9-liter crystallizer and the mini-nucleator

were virtually eliminated when 6-mm glass beads were added to the latter vessel.

6. Relative crystal habit for $CaSO_3 \cdot 1/2H_2O$ is unaffected by changes in precipitation rate between 182.2 and 61.9 mg/min-l.
7. The present design of flue-gas scrubbers yields a product which has a weight-average size approximately 30% less than that from an equivalent MSMPR. This difference is due to recycle of fines from the clarifier in current industrial configurations.
8. Scrubber product mass-average size was predicted to increase approximately 50% through the use of the proposed Double Draw-Off hold-tank configuration. Mass-average size might be increased an additional 80% by improvements in clarifier design and operation.

APPENDIX

METASTABILITY DATA

C = crystals detected

NC = no crystals detected

No Chemical Additive:

$NaHSO_3$ Pump Run Time (sec)	Run # 1	2	3	4	5	6	7	8	9	10	11	12	13	14	15	16	17	18	19	N+1
70	--	C	--	--	--	--	--	--	--	--	--	--	--	--	--	--	--	--	--	--
85	--	--	--	--	--	--	--	--	--	--	--	--	C	--	C	--	C	--	--	--
80	--	--	C	--	--	C	--	C	--	C	--	NC	--	NC	--	NC	--	C	--	--
75	--	--	--	--	NC	--	NC	--	NC	--	NC	--	--	--	--	--	--	--	C	--
70	NC	--	--	NC	--	--	--	--	--	--	--	--	--	--	--	--	--	--	--	X

30 ppm Citric Acid:

$NaHSO_3$ Pump Run Time (sec)	Run # 4	5	6	7	8	9	10	11	12	13	14	15	16	17	18	19	N+1
150	--	C	--	--	--	--	--	--	--	--	--	--	--	--	--	--	--
145	--	--	--	--	--	--	--	--	--	--	--	--	--	--	--	--	--
140	--	--	--	--	--	--	--	--	--	--	--	--	--	--	--	--	--
135	--	--	--	--	--	--	--	--	--	--	--	--	--	--	--	--	--
130	--	--	C	--	C	--	--	--	--	--	--	--	--	--	--	--	--
125	--	--	--	NC	--	C	--	--	--	--	--	C	--	--	--	C	--
120	--	--	--	--	--	--	C	--	C	--	NC	--	C	--	NC	--	X
115	--	--	--	--	--	--	--	NC	--	NC	--	--	--	NC	--	--	--
110	NC	--	--	--	--	--	--	--	--	--	--	--	--	--	--	--	--

< 30 ppm Sodium Oleate:

$NaHSO_3$ Pump Run Time (sec)	Run #																					
	2	3	4	5	6	7	8	9	10	11	12	13	14	15	16	17	18	19	20	21	22	N+1
115	--	--	--	--	--	C	--	--	--	--	--	--	--	--	--	--	--	--	--	--	--	--
110	C	--	--	--	--	--	C	--	--	--	--	--	--	--	--	--	--	--	--	--	--	--
105	--	--	--	--	NC	--	--	C	--	--	--	--	--	--	--	--	--	--	--	--	C	--
100	--	--	--	NC	--	--	--	--	C	--	--	--	--	C	--	C	--	C	--	NC	--	X
95	--	--	NC	--	--	--	--	--	--	--	--	--	NC	--	NC	--	NC	--	NC	--	--	--
90	--	NC	--	--	--	--	--	--	--	C	--	NC	--	--	--	--	--	--	--	--	--	--
85	--	--	--	--	--	--	--	--	--	--	NC	--	--	--	--	--	--	--	--	--	--	--

30 ppm Gelatin:

$NaHSO_3$ Pump Run Time (sec)	Run #															
	1	2	3	4	5	6	7	8	9	10	11	12	13	14	15	16	N+1
110	--	--	--	--	--	C	--	--	--	--	--	C	--	--	--	C	--
105	--	--	--	--	NC	--	C	--	--	--	NC	--	C	--	NC	--	X
100	C	--	--	NC	--	--	--	C	--	NC	--	--	--	NC	--	--	--
95	--	--	NC	--	--	--	--	--	NC	--	--	--	--	--	--	--	--
90	--	NC	--	--	--	--	--	--	--	--	--	--	--	--	--	--	--

30 ppm Adipic Acid:

$NaHSO_3$ Pump Run Time (sec)	Run # 1	2	3	4	5	6	7	8	9	10	11	12	13	14	15	16	17	N+1
120	--	--	--	--	--	--	C	--	--	--	--	--	--	--	C	--	--	--
115	--	--	--	--	--	NC	--	C	--	--	--	--	--	NC	--	C	--	--
110	--	--	--	--	NC	--	--	--	C	--	C	--	NC	--	--	--	C	--
105	--	--	--	NC	--	--	--	--	--	NC	--	NC	--	--	--	--	--	X
100	C	--	NC	--	--	--	--	--	--	--	--	--	--	--	--	--	--	--
95	--	NC	--	--	--	--	--	--	--	--	--	--	--	--	--	--	--	--

20.9 ppm Adipic Acid:

$NaHSO_3$ Pump Run Time (sec)	Run # 10	11	12	13	14	15	16	17	18	19	N+1
85	C	--	C	--	--	--	--	--	--	--	--
80	--	NC	--	C	--	--	--	--	--	C	--
75	--	--	--	--	C	--	--	--	NC	--	X
70	--	--	--	--	--	C	--	NC	--	--	--
65	--	--	--	--	--	--	NC	--	--	--	--

30 ppm NMTP:

$NaHSO_3$ Pump Run Time (sec)	Run # 16	17	18	19	20	21	22	23	24	25	26	N+1
440	--	--	C	--	--	--	--	--	--	--	--	--
420	C	--	--	C	--	C	--	--	--	--	--	--
400	--	NC	--	--	NC	--	C	--	--	--	--	--
380	--	--	--	--	--	--	--	--	C	--	--	--
360	--	--	--	--	--	--	--	NC	--	C	--	X
340	--	--	--	--	--	--	--	--	--	--	NC	--

< 49.8 ppm SDBS:

$NaHSO_3$ Pump Run Time (sec)	Run # 3	4	5	6	7	8	9	10	N+1
80	--	--	--	C	--	--	--	C	--
75	C	--	NC	--	C	--	NC	--	X
70	--	NC	--	--	--	NC	--	--	--

42 ppm EDTA:

$NaHSO_3$ Pump Run Time (sec)	Run #								
	1	2	3	4	5	6	7	8	N+1
100	C	--	C	--	--	--	--	--	--
95	--	NC	--	C	--	--	--	--	--
90	--	--	--	--	C	--	C	--	X
85	--	--	--	--	--	NC	--	NC	--

LIST OF REFERENCES

Brownlee, K. A., J. L. Hodges, Jr., and M. Rosenblatt, J. Amer. Stat. Assoc., 48, 262 (1953).

Burton, W. K., N. Cabrera, and F. C. Frank, Phil. Trans. Roy. Soc. (London), A243, 299 (1951).

Clontz, N. A., and W. L. McCabe, Chem. Engr. Progr. Symp. Ser., 67, 110 (1971).

Coltharp, W. M., N. P. Meserole, B. F. Jones, K. Schwitzgebel, R. S. Merrill, G. L. Sellman, C. M. Thompson, and D. A. Malish, Chemical/Physical Stability of Flue Gas Cleaning Wastes, Radian Corp., EPRI-FP-671, January (1979).

Corbett, W. E., O. W. Hargrove, and R. S. Merrill, A Summary of the Effects of Important Chemical Variables upon the Performance of Lime/Limestone Wet Scrubbing Systems, Radian Corp., EPRI-FP-639, December (1977).

Crowe, J. L., and S. K. Seale, Full-Scale Scrubber Sludge Characterization Studies, TVA, EPRI-FP-942, January (1979).

Dixon, W. J., and A. M. Mood, J. Amer. Stat. Assoc., 43, 109 (1948).

Edwards, L. O., Calcium Sulfite Crystal Sizing Studies, Radian Corp., EPA-600/7-79-192, August (1979).

Epstein, M., EPA Alkali Scrubbing Test Facility: Summary of Testing Through October 1974, Bechtel Corp., EPA-650/2-75-047 (1975).

Epstein, M., C. C. Leivo, C. H. Rowland, and S. C. Wang, Test Results from the EPA Lime/Limestone Scrubbing Test Facility, Bechtel Corp., Proc. Flue Gas Desulfurization Symposium, New Orleans (1973).

Etherton, D. L., Experimental Study of Calcium Sulfate (Gypsum) Crystallization from Stack-Gas Liquors, M.S. Thesis, University of Arizona, Tucson (1980).

Jones, B. J., P. S. Lowell, and F. B. Meserole, Experimental and Theoretical Studies of Solid Solution Formation in Lime and Limestone SO_2 Scrubbers, Radian Corp., EPA-600/2-76-273a, October (1976).

Matuchová, M., and J. Nývlt, Kristall und Technik, 11, 149 (1976).

McCall, T., and M. E. Tadros, Effects of Additives on Morphology of Precipitated Calcium Sulfate and Calcium Sulfite, unpublished manuscript, Martin Marietta Corp., Baltimore (1979).

Melia, T. P., J. Appl. Chem., 15, 345 (1965).

Michaels, A. S., P. L. T. Brian, and W. F. Beck, Cinemicrographic Studies of Single Crystal Growth: Effects of Surface Active Agents on Adipic Acid Crystals Grown from Aqueous Solution, Proc. IVth International Conference of Surface Active Substances, Brussels (1964).

Michaels, A. S., and A. R. Colville, Jr., J. Phys. Chem., 64, 13 (1960).

Nuttall, H. E., Computer Simulation of Steady State and Dynamic Crystallizers, Ph.D. Dissertation, University of Arizona (1971).

Nývlt, J., R. Rychlý, J. Gottfried, and J. Wurzelová, J. Crystal Growth, 6, 151 (1970).

Otmers, D., J. Phillips, C. Burklin, W. Corbett, N. Phillips, and C. Shelton, A Theoretical and Experimental Study of the Lime/Limestone Wet Scrubbing Process, Radian Corp., EPA-650/2-75-006, December (1974).

Ottens, E. P. K., Nucleation in Continuous Agitated Crystallizers, Ph.D. Dissertation, Delft University, The Netherlands (1973).

Randolph, A. D., and D. Etherton, Study of Gypsum Crystal Nucleation and Growth Rates in Simulated Flue Gas Desulfurization Liquors, EPRI-CS-1885, June (1981).

Randolph, A. D., and M. A. Larson, Theory of Particulate Processes, Academic Press, New York (1971).

Sibert, W., Dynamic Crystal Size Distribution Simulation and Control Strategies for Crystallizers Equipped with Fines Destruction and Product Classification, M.S. Thesis, University of Arizona, Tucson (1982).

Vaden, E. D., Effects of Particle Size Classification on Gyptum Size Distribution in Simulated Stack-Gas Scrubbing Liquors, M.S. Thesis, University of Arizona, Tucson (1981).

Van Rosmalen, G. M., Scale Prevention, Delft University Press, The Netherlands (1981).

Wey, J. S., and R. Jagannathan, AIChE J., 28(4), 697 (1982).